

MODELS FOR INVESTIGATING FUNCTIONAL ROLES OF OSTEOPONTIN:  
CHARACTERIZATION OF ANTI-OPN MONOCLONAL ANTIBODIES

by

DANA M. CIFELLI

A thesis submitted to the

Graduate School-New Brunswick

Rutgers, The State University of New Jersey

And

The Graduate School of Biomedical Sciences

University of Medicine and Dentistry of New Jersey

In partial fulfillment of the requirements

For the degree of

Master of Science

Graduate Program in Microbiology and Molecular Genetics

Written under the direction of

Dr. David T. Denhardt

And approved by

---

---

---

---

New Brunswick, New Jersey

May, 2009

## **ABSTRACT OF THE THESIS**

**Models for Investigating Functional Roles of Osteopontin:**

**Characterization of Anti-OPN Monoclonal Antibodies**

**By DANA M. CIFELLI**

Thesis Director:  
David T. Denhardt

Osteopontin is an integrin-binding phosphorylated glycoprotein. It is found in many tissues and can be found in all body fluids. It is associated with several cellular processes such as cell survival, cancer progression and stress response. These particular cellular processes were of interest in my research.

This thesis is divided into two parts. Part I being about the purification of OPN and characterization of anti-OPN monoclonal antibodies. In order to accomplish part I of this thesis, OPN was purified by ion-exchange and desalting chromatography, and analyzed by SDS-PAGE followed by Coomassie Blue staining. The methods for purifying anti-OPN mAbs from hybridomas by ascites consisted of ammonium sulfate precipitation, ion-exchange chromatography, and protein A/G purification. Anti-OPN mAbs were characterized by SDS-PAGE analysis, Western blotting and ELISAs. The results from these analyses were then compiled into our database. The OPN and mAbs that were made were used in several experiments by my fellow lab mates and me.

The second part of my thesis was to investigate potential models for characterizing the functional roles of OPN. This was accomplished by studying cell survival with human umbilical vein endothelial cells (HUVECs) and cancer cell

phenotypes with the pancreatic cancer cell line HS766T. Flow cytometry was used to analyze cell survival in HUVECs. Transfection with specific plasmids designed to increase or decrease OPN expression was used to modulate the cancer cell phenotype of HS766T cells.

In conclusion, I was able to successfully generate several pure stable preparations of OPN and anti-OPN mAbs. Also, I was able to reproduce cell survival in HUVECS by OPN a few times but because it was not consistently reproducible, I was unable to tests the effects of mAbs on the survival of HUVECs by OPN. Also, since our research was already successfully carried out and published by another group, I decided not to purse this project further. Lastly, I was able to create several clones of HS766T that exhibited increased or decreased OPN expression as determined by Real-Time PCR analysis.

## ACKNOWLEDGEMENTS

I would like to acknowledge first and foremost Dr. David Denhardt my thesis advisor. If it were not for his compliments, positive attitude, and his compassion for our lab and my research, I do not feel that I would have succeeded in my research. He provided a great learning environment as well as a comfortable working environment. The easy-going relationship between my thesis advisor and I always made it a pleasure to come to lab. There were several students in my lab that showed continual support by critiquing and analyzing my results. These students are Katie Jaques, Sunanda Baliga, Tanya Gordonov, Jen Luo and Chris Kazanecki.

My thesis committee consisting of Dr. Yacov Ron, Dr. Chiann-Chyi Chen and Dr. David Axelrod, I owe a great amount of thanks to for their guidance and critical analysis of my thesis. A special thanks has to be given to Dr. Yacov Ron and his lab for their generosity in providing us with ascites. The mAbs purified from the ascites fluid were used in several of my experiments. In addition, I would like to thank Dr. Arafat and her students for their financial and academic support in the pancreatic cancer project.

I would also like to thank my family who has supported me through my entire academic career. It has been a long 20 years of education and my family has been there for every minute of it. From the frustrations, the awards, the graduations and the many nights where my Mom would shove my food under the door because I had so much work to do, they have been there for it all. Special attention has to be given to my mother whose perseverance and constant reassurance has made this process immensely easier. Since I was a child my father always called me his little Madam Curie and it was his dream for me that made me want to pursue science and a graduate degree. My fiancé

Patrick has been a major supporter of my education as well as my career choice. He would proofread my papers, take me to all of my meetings and offered a comforting hand when I became stressed. Although my academic career at Rutgers may be over, I know I will continue to grow, study and apply everything that I have learned over the past two decades to my forthcoming career.

## TABLE OF CONTENTS

ABSTRACT.....	ii
ACKNOWLEDGMENTS.....	iv
LIST OF TABLES.....	vii
LIST OF FIGURES.....	viii
INTRODUCTION.....	1
MATERIALS & METHODS.....	16
RESULTS.....	26
DISCUSSION.....	48
REFERENCES.....	53

## LIST OF TABLES

<b>Table 1.</b> Representative Clones.....	46
<b>Table 2.</b> Up-Regulation or Down-Regulation of Clones Based on Fold Difference.....	47

## LIST OF FIGURES

<b>Figure 1.</b> OPN Gene.....	2
<b>Figure 2.</b> OPN Signaling.....	3
<b>Figure 3.</b> Conductivity of OPN Fractions.....	27
<b>Figure 4.</b> Analysis of Fractions Where OPN Eluted.....	28
<b>Figure 5.</b> Monoclonal Antibodies Purified from Conditioned Media.....	29
<b>Figure 6.</b> SDS PAGE Coomassie Blue Gel of Antibodies Purified from Ascites.....	30
<b>Figure 7.</b> Western Blot to Determine if an IgM is Produced by 67F7.....	31
<b>Figure 8.</b> Elisa of mAbs Made from Ascites Fluid.....	32
<b>Figure 9.</b> FACS Results of HUVEC Cells in Apoptosis.....	34
<b>Figure 10.</b> DNA Content Analysis.....	35
<b>Figure 11.</b> Cytokine Assay of HUVEC Cells.....	36
<b>Figure 12.</b> Relation of mRNA Levels Tested with House Keeping Gene.....	38
<b>Figure 13.</b> Relation of mRNA Levels Tested with OPN Primer.....	39
<b>Figure 14.</b> SDS-PAGE Analysis of the Parent Cell Serum-Free Conditioned Medium...40	
<b>Figure 15.</b> GAPDH Control Amplification Plot.....	41
<b>Figure 16.</b> Roche OPN Primer Amplification Plot.....	42
<b>Figure 17.</b> GAPDH Control - Dissociation (Melt) Curve.....	43
<b>Figure 18.</b> Roche OPN Primer – Dissociation (Melt) Curve.....	44
<b>Figure 19.</b> Cell Migration Assay of HS766T Parent Cells.....	48
<b>Figure 20.</b> Cell Migration Assay of ASPC-1 Parent Cells.....	49



## **Chapter 1**

### **Introduction**

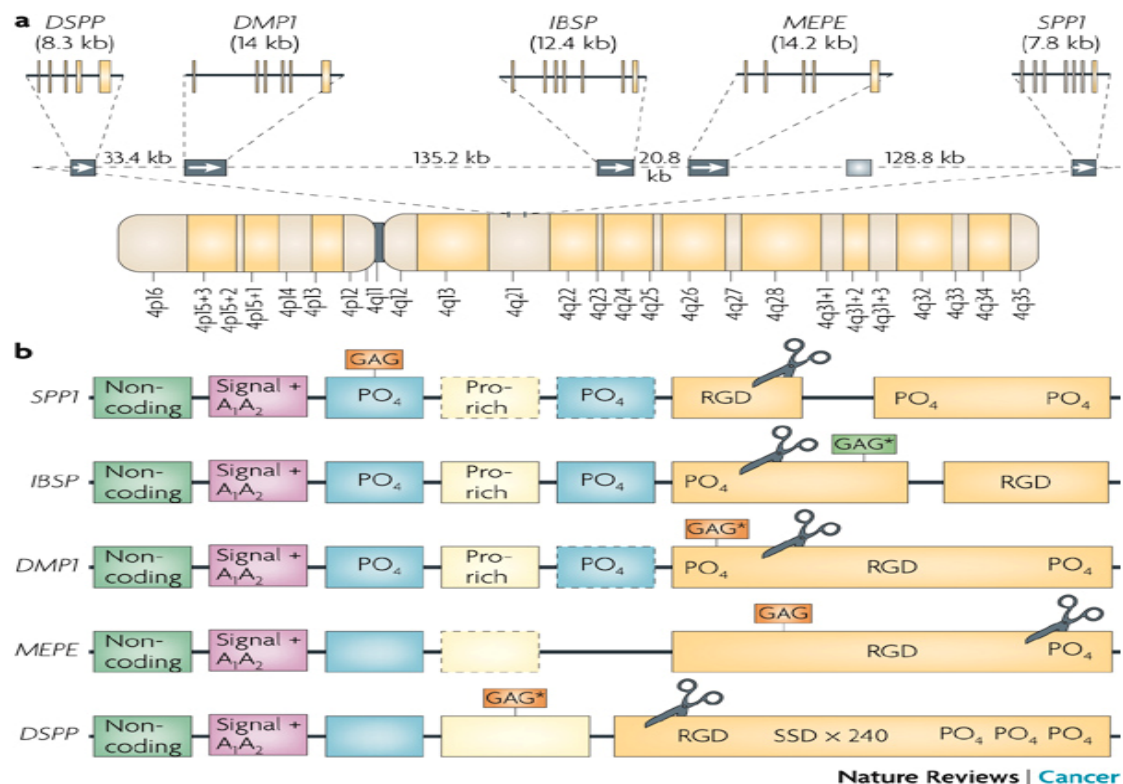
Osteopontin (OPN), also known as secreted phosphoprotein 1 (SPP1) is a highly phosphorylated glycoprotein that functions both as a cytokine and a noncollagenous bone matrix protein [Yumoto et al., 2002]. It is found in a variety of tissues including bone, brain, kidney and immune organs. It is present in all body fluids including blood, milk and urine. OPN is a multifunctional, structurally heterogeneous protein that is associated with several cellular processes such as cell adhesion, proliferation, survival, and migration; it is also necessary for bone remodeling.

OPN expression has become a vital component in understanding the regulation of cancer metastasis and has been suggested to be a potential therapeutic target [Wai and Kuo, 2008]. For example, the mAb 23C3D3 recognizes a phage that displays the peptide WLNPDP and it can inhibit OPN-induced lymphocyte survival, migration and proliferation. This epitope of OPN can be used as a therapeutic target for the treatment of T-cell mediated immune diseases [Cao et al., 2008]. This glycoprotein is very influential during the development of natural killer (NK) cells. One study has shown that the absence of OPN in the cellular microenvironment caused a significant reduction in the NK cell population whereas the absence of intrinsic intracellular OPN did not cause a reduction [Chung et al., 2008].

#### **1.1 Gene Structure and Protein**

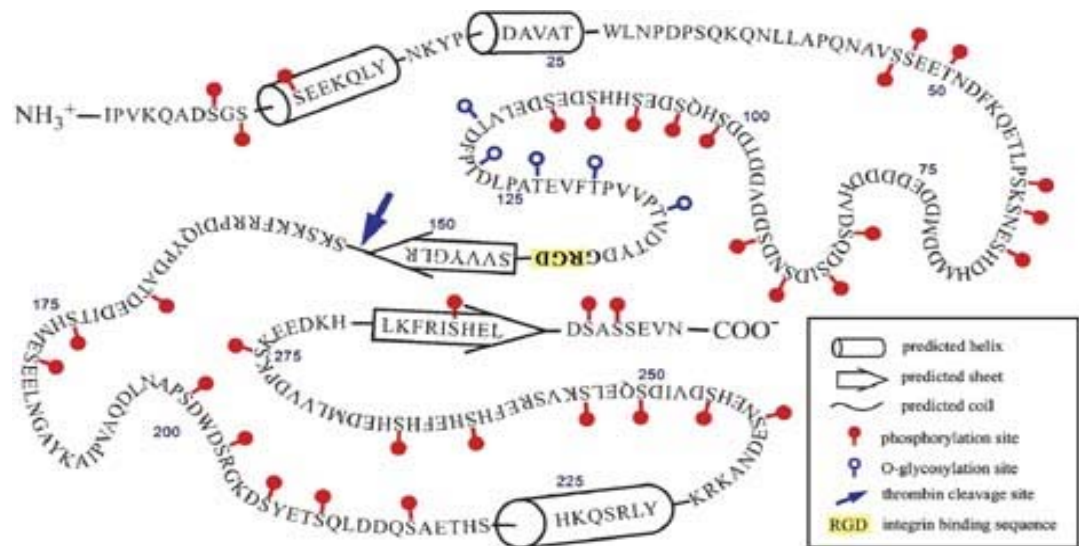
The OPN gene maps to the long arm of human chromosome 4 (4q21-25) [Sodek et al., 2000]; the protein is 317 amino acids in length. The OPN gene consists of 6 coding exons and one non-coding exon [Craig and Denhardt, 1991; Hijiya et al., 1994] (Fig.1).

There is a thrombin cleavage site and a RSK sequence that is conserved in many species (Fig.2). This conserved sequence suggests that thrombin cleavage could play a role in how OPN operates [Rangaswami et al., 2006]. OPN lacks extensive secondary structure, and its primary sequences can vary. The areas that are conserved can be found in regions where there may be  $\alpha$  helix and  $\beta$  sheet structures and between the GRGDS and thrombin cleavage sites [Kazanecki et al., 2007]. The SDS-PAGE molecular weight varies between 50-70kDa due to the differences in electrophoretic conditions and post-translational modifications.



[Bellahcene et al., 2008]

**Figure 1. OPN Gene.** *SPP1*, part of the SIBLING family, has 6 coding regions and one non-coding region in humans and mice. It is found on the long arm of the human chromosome 4 (4q21-25). The scissors show where the protein is cleaved by thrombin. The cleavage results in exposure of the cryptic binding site (see 1.5 below). *SPP1* is 7.8kb.



[Kazanecki et al., 2007]

**Figure 2. OPN Signaling.** The RGD integrin binding sequence and the thrombin cleavage site are indicated. The cryptic cleavage site in humans, "SVVYGLR" is also shown but can only be revealed through thrombin cleavage.

There are three splice variants of human OPN that exist and only 1 variant in mouse. In humans OPNa, the full-length molecule, is the most common splice variant. OPNc has exon 4 spliced out and OPNb has exon 5 spliced out. This has been detected in glioma cells [Saitoh et al., 1995]. The absence of exon 4 in OPNc supports anchorage independent growth of cancer cells [Mirza et al., 2008]. OPNa likely affects the equilibrium due to that fact that a portion of the secreted protein aggregates. This is supported by He et al.'s findings of aggregation of OPNa, resulting in enhanced cell adhesion at physiologic calcium concentrations. OPNb and OPNc promote metastasis while OPNa does not [He et al., 2006].

## 1.2 Tissue Distribution

Cells in several tissues such as bone, brain, and kidneys express OPN. OPN is in all biological fluids including urine, milk, and seminal fluid. Patients who have tumors or autoimmune diseases have higher concentrations of plasma OPN [Singhal et al., 1997].

OPN can be induced in carcinomas and its outcome can be related to the metastasis of the cancerous cells [Chambers et al., 1992]. During pathological situations, inflammation or injury, OPN expression is up-regulated in many cell types. Chambers et al. (1992) have hypothesized that this is due to the increase in number of macrophages and T-lymphocytes during these situations.

### **1.3 Regulation of Expression**

Several cytokines, hormones and growth factors can affect the expression of OPN. These and other factors can also impact on how OPN mRNA is processed, the rate of transcription and the post-translational modifications that occur. Glucocorticoids cause an increase in OPN expression in rat bone marrow cell culture. However Vitamin D3, which is a strong stimulator of OPN synthesis in bone cells and epidermal cell lines, will cause OPN expression to be lower if there is a vitamin D3 deficiency [Chen et al., 1999]. Glucocorticoids can also cause an increase in OPN expression in bone cells. Epidermal growth factors (EGF) can also up-regulate OPN expression.

OPN is normally up-regulated by some hormones and cytokines whereas bisphosphonates suppress the regulation in bone [Sodek et al., 2000]. An increased expression of OPN is caused by the regulation of the transactivation of cis-acting elements in the gene promoter. A recent demonstration suggests that inorganic phosphates can regulate OPN gene transcription in cementoblasts through a functional glucocorticoid receptor [Fatherazi et al., 2009]. Also, T-bet which assembles expression of T cells, is important in the development of Th 1 T cells. OPN gene expression is regulated by T-bet. The distorting of T cells towards Th 1 differentiation is due to a dependence of T-bet on OPN expression [Shinohara et al., 2005].

#### **1.4 Post-Translational Modifications (PTM)**

Post-translation modifications such as phosphorylation and O-glycosylation can alter the biological functions of OPN. Phosphorylation and sulfation can change the surface character of OPN to higher negative charges, while glycosylation limits the flexibility of OPN [Sodek et al., 2000]. Phosphorylation of OPN on serine and threonine residues is catalyzed by members of the casein kinase [Saavedra et al., 1995]. Glycosylation occurs regularly and in most mineralized tissues sulphation occurs mostly in the highly phosphorylated form of OPN. Several post-translational modifications are conserved across species but the degree of modification to the protein varies depending on the tissue and cell type. Multiple forms of OPN exist in normal and transformed cells. These forms shed some light into the structure and function of OPN because of the conserved region of the RGD site, thrombin cleavage site, and serine/threonine phosphorylation sites [Sodek et al., 2000]. In bovine milk OPN there are 27 phosphoserine and 1 phosphothreonine residue. In human milk OPN there are 34 phosphoserine and 2 phosphothreonine residues [Christensen et al., 2007]. Both of the milk-derived OPNs show that phosphorylation residues are often in clusters of three to five residues. Bovine mammary gland OPN contains 3 O-glycosylations and the human milk OPN has 5 O-glycosylations. Neither of these milk-derived OPNs have N-glycosylations [Christensen et al., 2007]. To date, it has been reported that rat kidney and human bone OPN have N-glycosylations [Masuda et al., 2000].

#### **1.5 Signaling through Integrins and CD44 Variants**

Some integrins that intact OPN interacts with include  $\alpha v \beta 3$ ,  $\alpha v \beta 5$ ,  $\alpha v \beta 1$ , and CD44 splice variants [Yokosaki et al., 2005]. OPN typically binds to integrin receptors

via the RGD motif of (Fig. 2). The RGD-binding integrin  $\alpha v \beta 3$  has been shown to be a primary receptor for OPN binding in many types of cells. OPN- $\alpha v \beta 3$  is important in mineral resorption, osteoclast migration, smooth muscle cell migration and adhesion. OPN also has a cryptic integrin attachment motif, “SVVYGLR” in humans and “SLAYGLR” in mouse [Yamamoto et al., 2007]. This site sequence is only accessible after the cleavage between the R and S residues of OPN by thrombin (Fig. 2). This cryptic cleavage site is used by  $\alpha 9 \beta 1$ ,  $\alpha 8 \beta 1$ , and  $\alpha 4 \beta 1$  in cell adhesion [Barry et al., 2000]. In addition to the cryptic cleavage site, OPN also has two heparin-binding sites, an aspartate-rich region and a region near the C terminus that binds CD44 variants. OPN interacts with CD44 variants v6 and v7, activating transcription of the CD44 gene in human tumor cells [Khan et al., 2005].

## **1.6 Apoptosis**

Apoptosis, in contrast to necrosis, is when cells die in a regulated fashion and not by uncontrolled cell lysis. This form of programming has been evolutionarily conserved from worms to humans [Khan et al., 2002]. Apoptosis has several functions that include cell elimination, maintaining homeostasis, development of organs and lymphocyte interactions. There are several intracellular/extracellular apoptotic signals that a cell releases when it is stressed and it is these signals that can lead to cell death by apoptosis. Some extracellular signals include hormones, toxins, growth factors, nitric oxide and cytokines. A cell can become stressed for various reasons including viral infection, radiation, heat and nutrient deficiency. Regulatory proteins are the main way that the apoptosis signals are joined to the death pathway. Three major factors contribute to the biochemical process of apoptosis. These factors are the Bcl-2 family proteins, caspases,

and the Apaf-1/CED-4 protein [Ashkenazi, 2008]. The two main biochemical pathways of caspase activation during apoptosis are the cell surface death receptor pathway and the mitochondria initiated pathway.

### **1.6.1 Mitochondria Initiation Pathway and Apoptosis**

Secondary mitochondrial-derived activator of caspases (SMACs) are mitochondrial proteins that are released into the cytosol [Ashkenazi, 2008]. SMACs bind to inhibitor of apoptosis proteins (IAPs), which then makes these proteins turn off. When the IAPs are shut off, they cannot stop apoptosis from proceeding. The caspases, which help in cell protein degradation, are controlled by the IAPs. During regulation of blood clotting, caspases exist as inactive proenzymes. When apoptosis occurs, these enzymes become activated through proteolytic processes that cleave a single protein precursor into large and small fragments, which make up the active enzyme.

When cytochrome c is released from the mitochondria, it binds to Apaf-1 and ATP and then to pro-caspase-9. This produces the apoptosome. The Bcl-2 family of proteins can inhibit or promote apoptosis through the mitochondria apoptosis-induced channel (MAC) even though cytochrome c is being released from the mitochondria [Ashkenazi, 2008].

### **1.6.2 Direct Signal Transduction in Apoptosis**

Tumor necrosis factors (TNF) are cytokines that are involved in direct signal transduction in apoptosis. The TNF-induced model and the Fas-Fas ligand-mediated model are the two mechanisms that are involved in apoptosis and that involve action of TNFs. TNF receptor-associated death domain (TRADD) and Fas-associated death domain protein (FADD) are domains that are involved in caspase activation when TNF

binds to TNF-R1 (Chen et al., 2002).

The death-inducing signaling complex (DISC) is formed because of the Fas receptor binding to the Fas ligand. First there is a ligand-induced receptor trimerization followed by a recruitment of intracellular receptor-associated proteins and lastly the initiation of caspase activation. The DISC houses the FADD, caspase-10 and caspase-8. Apoptosis can progress by the release of pro-apoptotic factors from the mitochondria. The Fas-DISC initiates a feedback loop that causes the release of pro-apoptotic factors and causes an increase in caspase-8 [Wajant et al., 2005].

Members in the Bcl-2 family of proteins generate a balance that consists of pro-apoptotic and anti-apoptotic factors go along with the activation of the Fas and TNF-R1. In order for caspase activators to be released from the mitochondrial membrane, the membrane must first be made permeable.

There are three mechanisms that regulate the cell surface death receptor activation. One mechanism is that procaspase recruitment is obstructed and/or activation of DISC is prevented. Another mechanism involves the expression of decoy receptors for TRAIL. The last mechanism, involves a direct inhibition of the proteolytic activation of the initiator procaspases.

### **1.6.3 Osteopontin and Apoptosis**

Since the initial report of Denhardt et al. (1995), numerous studies have indicated that OPN is capable of suppressing apoptosis. The way in which OPN facilitates survival of cells by suppressing apoptosis depends on the cell type. In primary human umbilical vein endothelial cells (HUVECs), OPN facilitates the survival of these stressed growth factor-deprived cells. Here OPN suppresses apoptosis and DNA fragmentation by



interacting with  $\alpha v\beta 3$  integrin and the activation of NF- $\kappa$ B. OPN acts as a cytokine and engages unoccupied integrin receptors in order to inhibit the induction of apoptosis in the growth factor deprived HUVECs [Khan et al., 2002]. Bredeisen et al., 1998 suggests that apoptosis of cells will be induced if certain receptors are not engaged by their ligands.

In type II collagen-activated murine T cells and synovial T cells from rheumatoid arthritis patients, OPN prevented cell death by inhibiting apoptosis. An anti-OPN mAb, 23C3, was effective in promoting apoptosis of the activated T cells by interfering with NF- $\kappa$ B, altering the apoptotic proteins, and the antiapoptotic protein Bcl-2 [Fan et al., 2008].

OPN can also promote tumor growth and metastasis through inhibition of apoptosis. One study has found that if OPN expression is down-regulated then the metastasis of hepatocellular carcinoma growth is reduced because this causes apoptosis to be induced [Zhao et al., 2008]. These results were achieved by using a short hairpin RNA-mediated gene silencer. The reduction in OPN levels caused the inhibition of hepatocellular carcinoma growth, anchorage and adhesion growth, and tumorigenicity. It also resulted in suppression of  $\alpha v$ ,  $\beta 1$ , and  $\beta 3$  integrin expression and inhibition of Bcl-2/Bcl-xL expression.

## **1.7 OPN and Cancer**

OPN plays a crucial role in determining the metastatic potential of various cancers [Rangaswami et al., 2006]. It is expressed at high levels in tumors and the surrounding stroma of numerous cancers, including those of the liver, breast, stomach, lung and colon. Higher levels of plasma OPN have been correlated with advanced-stage lung, breast, colon and prostate carcinomas [Hotte et al., 2002]. OPN, as well as other members of the

SIBLING family, are greatly expressed in several cancer cells and their prevalence directly correlates with the tumor grade [Rangaswami et al., 2006].

OPN can prevent apoptosis in murine B-cells through the inactivation of the PI 3-kinase/Akt pathway [Lin and Yang-Yen, 2001]. In the ECM, OPN can up-regulate pro-MMP-2 expression in a NF- $\kappa$ B-dependent manner [Phillip et al., 2001]. OPN enables tumor cells to resist host-immune cells, causes neovascularization, and stimulates cell migration. These aforementioned unique features of OPN make it a great mediator in all types of cancer.

### **1.7.1 OPN and Its Role in Hepatocellular Carcinoma**

Hepatocellular carcinoma (HCC) is an extremely dangerous carcinoma of the liver that is being reported at a steady rate worldwide [Blum, 2005]. Identification of the primary contributors to the metastatic cascade may present significant opportunities for reducing the severity of this disease through new therapeutic techniques. OPN expression can be used to foresee late-stage, high grade and early-recurrence HCC [Pan et al., 2003]. Furthermore, OPN expression is highly correlated with tumor reappearance and reduced patient survival following orthotopic liver transplantation [Wang et al., 2005].

Ye et al. (2003) discovered OPN as a predictive indicator for HCC and a molecular target of the HCC metastatic phenotype. OPN and MMP-9 protein levels correlate with the degree of metastasis and tumor malignancy in numerous cancers [Fedarko et al., 2001]. Current research conducted by Takafuji et al. (2007) proposed an OPN/MMP-9 interaction that is related to intra-hepatic tumor cell invasion in HCC. Furthermore, this study proposed that proteolytic exposure of a cryptic non-RGD region

of OPN is crucial to facilitate cellular invasion. Through this research a distinctive 5-kDa OPN fragment was identified that correlates with cellular invasion via CD44 and a metastatic potential in three tested HCC cell lines. This study suggests the presence of a mechanism by which OPN and MMP-9 function in unison to promote early tumor cell invasion *in vivo* and evoke a novel peptide approach for HCC treatment. The OPNc splice variant appears to be uniquely sensitive to cleavage by MMP-9. That cleavage releases a distinct region of OPN called OPN 5-kDa that is central for HCC cellular invasion and seems to positively correlate with metastatic potential.

### **1.7.2 OPN and Breast Cancer**

Most deaths from breast cancer are a result of distant metastases rather than primary tumor burden. Recent research conducted by Cook and colleagues found that OPN over-expression in a breast cancer cell line changed the gene expression profile, including changes in genes typically associated with multiple stages of tumor formation [Cook et al., 2005]. These data suggest that OPN may significantly contribute to early tumor progression as well as malignant behavior. These findings were supported by subsequent research conducted by Shevde and colleagues [Shevde et al., 2006]. They found that the expression of OPN correlates with the aggressive phenotype of breast cancer cells. In order to properly assess the role of OPN in carcinomas, Shevde et al. (2006) knocked down the expression of endogenous OPN in metastatic MDA-MB-435 human breast carcinoma cells using RNA interference. Through using this technique they were not only able to show the widely reported roles of OPN in late stages of tumor progression, but also able to provide functional evidence that OPN contributes to breast tumor growth as well.

Research conducted by He and colleagues found that while OPN is expressed at high levels by various cancers, it can also provoke cellular immunity and could boost anti-tumor protection by cytotoxic T lymphocytes when derived from host cells [He et al., 2006]. By researching breast cancer cells, this group was able to classify the mechanism of alternative splicing. They proposed that this mechanism is utilized by cancer cells to alter the structure and function of OPN, leading to increased anchorage independence. It was found that OPNc strongly supports anchorage-independent growth. To the contrary, OPNa has a transitional effect, possibly reflecting an equilibrium, in which a segment of the secreted product aggregates, with the remaining soluble portion supporting soft agar clone formation. Thus, He and colleagues' data suggests that while the soluble form of OPN promotes metastasis, the aggregated form does not.

### **1.7.3 OPN and Pancreatic Cancer Due to Nicotine Exposure**

Although nicotine in itself is not carcinogenic, it exerts toxic effects on the pancreas. Tobacco stimulated-pancreatic cancer starts with a mixture of carcinogenic compounds and the nicotine present in cigarette smoke. Many of the components of this mixture have deleterious effects on the exocrine pancreas. The nicotine in this mixture forms carcinogenic *N*-nitroso compounds during processing, which causes pancreatic cancer in the Syrian golden hamster model of pancreatic carcinogenesis [Pour et al., 1981].

Numerous associations have been reported that suggest that there is a link between smoking behavior and genetic polymorphisms in genes that are responsible for nicotine metabolism. The CYP2A6 gene is polymorphic in the human population, with inter-individual differences in the concentrations of CYP2A6 protein. These differences

in concentrations can establish how functional the protein will be. Additional studies have found that individuals with genetically determined low or absent CYP2A6 activity have a lower risk of becoming smokers [Pianezza et al., 1998]. Thus, this suggests a role for CYP2A6 in nicotine tolerance and dependence. However, current literature suggests that CYP2A6 only affects nicotine metabolism among individuals who have high activity due to gene duplication [Saarikoski et al., 2000]. However, the influence of the low activity allele remains controversial.

OPN is essential to mediating the nicotine-induced changes in pancreatic cancer cell survival, proliferation, invasion, and migration in vitro [Arafat et al., 2006]. Nicotine has been shown to be involved in cancer cell proliferation and migration. Up until this point, exact mechanisms mediating these effects were unknown. Through data presented by Chipitsyna et al., (2009) it has been suggested that nicotine significantly up-regulates OPN transcription through induction of its promoter activity. This is important to note, due to the fact that OPN has been shown to induce cancer cell proliferation and migration. Thus, it is crucial to investigate whether OPN significantly contributes to changing cellular behavior after nicotine exposure.

## **1.8 Immunity**

### **1.8.1 Immune Defense System**

The host defenses consist of three layers [Lodish, et al., 2008]. Layer one consists of the mechanical and chemical layer. The mechanical layer includes the epithelia and the chemical layer includes a low pH of the gastric environment and antibacterial enzymes in tear fluid. Layer two is the innate immunity defense, which is mediated by the complement system and leukocytes. The innate system can be organized within minutes

to hours after pathogens have been found. Toll-like receptors detect the pathogens in the innate system. Layer three is controlled by the T and B lymphocytes by adaptive immunity. It can take days for full activation and deployment. B cells interact with intact antigens directly and T cells recognize cleaved forms of the antigen. The cleaved antigens can be found on antigen-presenting cells, which encode the major histocompatibility complex (MHC) that presents the antigen. The complementarity-determining region (CDR) confers the specificity of the antibody for an antigen.

### **1.8.2 Antigen Processing and Presentation**

The MHC is what accepts or rejects grafts and it can bind peptides in order to present them to antigen-specific receptors on T cells. Antigen processing and presentation is where a protein is cleaved into peptides, which are then displayed on the cell surface as MHC-peptide complexes. This process consists of 6 steps: (1) acquisition of antigen, (2) tagging the antigen for destruction, (3) proteolysis, (4) delivery of peptides to MHC molecules, (5) binding of peptide to the MHC molecule; and (6) display of the peptide-loaded MHC products. The epitope is that part of the peptide/antigen that is recognized by a specific antibody molecule.

### **1.8.3 Monoclonal Antibodies**

The different classes of antibodies are called isotypes. There are two light-chain isotypes and five heavy-chain isotypes. The immunoglobulin fold makes up the three dimensional structure. It consists of two  $\beta$  pleated sheets joined by a disulfide bond. Monoclonal antibodies (mAbs) are immunoglobulins that are identical and produced by one type of immune cell. These immune cells (hybridomas) are all clones of a single

parent cell. Hybridomas are produced by fusing immortal mouse myeloma cells with spleen cells from a mouse that has been immunized with a specific antigen such as OPN.

### **1.9 Relevance of Introduction to Thesis**

My first project was to purify OPN and characterize mAbs by SDS-PAGE gel, ELISAs, and Coomassie Blue staining. By learning such information as the size of OPN, PTMs, and what integrins OPN interacts with, I was able to interpret my purification results as well as the HUVEC results. My next project was to replicate HUVEC survival by OPN and then test how the addition of mAbs would affect how OPN protects HUVECs. In order to better understand HUVEC survival by OPN, I needed to learn how apoptosis works and how it can affect the expression of the cells. In my last project I investigated how OPN would affect the nicotine-induced changes in cell proliferation, invasion, survival and migration in vitro. A thorough background of how OPN operates in different types of cancer was important in order to understand how OPN may operate in pancreatic cancer.

## Chapter 2

### Materials and Methods

#### 2.1 Project 1: OPN Preparation

**2.1.1 Mouse OPN:** Ras-transformed fibroblasts (275-3-2) [Wu et al., 2000] were cultured in Dulbecco's Modified Eagle's Medium (DMEM) (Mediatech Inc., Herndon, Va) supplemented with 2mM L-glutamine, 100u/ml of penicillin, 100µg /ml streptomycin and 10% fetal bovine serum (FBS) (Hyclone, Logan, UT) in 10-cm plates. Cells were maintained at 37°C in 5.0% CO<sub>2</sub> for at least 24 hr until 80% confluency and were passaged by detaching with 0.05% trypsin-EDTA (Invitrogen, Grand Island, NY) and plated into several 10-cm plates. After the plates reached confluency, they were switched to regular DMEM without serum. These plates were washed with PBS before adding the DMEM with no serum. The medium was collected after 36 hr and was put in 50-ml conical tube and protease inhibitor cocktail (Sigma, St, Louis, MO) was added. The conditioned medium was collected by centrifugation, filter sterilized and then stored at 4°C.

**2.1.2 OPN Purification:** OPN was purified by ion-exchange column chromatography. The column was packed with Diethylaminoethyl Sepharose (DEAE) (GE Healthcare, Piscataway, NJ). The column was washed with 25 ml of 0.025M TrisCl pH 7.5/ 0.025M NaCl and then conditioned medium was added. The column was washed with 3 volumes of wash buffer. In order to set up the salt gradient, 50 ml of 0.05M TrisCl/ 0.1M NaCl and 50 ml of 0.475M NaCl/ 0.05M Tris-Cl were added to the two chambers of a mixing device. During the elution, 2 ml aliquots were taken at 7.5 min



intervals. The conductivity of the fractions was measured; OPN eluted around 300 $\mu$ S/cm.

**2.1.3 SDS-PAGE Analysis:** A 12% SDS-PAGE gel was prepared with a 4% stacking gel and the fractions that contained OPN were electrophoresed. The gel was then stained with Coomassie Blue for 90 min and destained for 60 min or until bands could clearly be distinguished. On occasion gels were silver-stained, which reveals OPN with greater sensitivity.

**2.1.4 OPN Preparation- Desalting:** The SDS-PAGE analysis results were used to determine which fractions had the most OPN. These fractions were pooled and passed through a 2-ml polystyrene desalting column (Thermo Scientific, Rockford, IL). The desalting procedure used was as per the manufacturer's instructions. The columns were equilibrated by gravity with 25 ml of 50 mM ammonium bicarbonate elution buffer. The samples were loaded with no more than 2.5 ml per column. The columns were eluted with 3.5 ml of elution buffer and 0.5 ml to 1.0 ml fractions were taken. The fractions containing OPN were assessed by the absorbance at 280 nm and were pooled, aliquoted, frozen at -70°C and then lyophilized.

## **2.2 Antibody Preparations and Characterization**

### **2.2.1 Culturing Cells and Collecting Antibodies from Conditioned Media:**

Because the hybridomas derived from the mice immunized with native human milk OPN (generously provided by Dr. Esben Sørensen, Aarhus University, Denmark) or phosphorylated peptides (courtesy Dr. Larry Steinman, Stanford University) had not been previously screened to identify those that made an anti-OPN mAb, I undertook to test the medium conditioned by those hybridomas to identify those that did indeed make an anti-

OPN mAb. The culturing of hybridomas was done using serum-free hybridoma medium (SFHM) (Invitrogen, Grand Island, NY). Typically two plates of one hybridoma each containing 25 ml SFHM were grown for about 2 weeks and then collected into a 50-ml conical. The cells were centrifuged and discarded. The supernatants (conditioned media) were filtered with a Pall Acrodisc 0.8/0.2  $\mu\text{m}$  filter (Cornwall, UK). A 1:100 dilution of 2.0% sodium azide and 1.0% thimerosol as added to each conditioned medium to ensure no fungal or yeast growth. The conditioned medium was concentrated using Centriprep YM-10 (Millipore Corporation, Billerica, MA) down to 1-2 ml each as per manufacturer's instructions.

**2.2.2 Purification of Antibodies from Conditioned Medium Using Protein G, Protein A, or Protein A/G Beads:** The concentrated antibodies were purified using one of the immobilized Proteins A, G or A/G (Pierce, Rockford, IL) following the manufacturer's instructions. The specific protein that was used to purify each antibody varied based on the binding affinity of the antibody to the immobilized protein. Immobilized protein A and A/G beads work best with a 0.01 M borate binding buffer with a pH 8.0. Protein G beads work best with a 1.5 M sodium acetate binding buffer with a pH 5.0. The procedures used for each of the immobilized protein beads are the same with the exception of the binding buffer.

Two-ml polystyrene columns (Thermo Scientific, Rockford, IL) were packed with the appropriate beads and then 5 ml of binding buffer was passed through followed by application of the antibody of interest diluted 1:1 with binding buffer. Columns were washed with 10-15 ml of binding buffer and then were eluted with 5 ml of elution buffer (0.1 M glycine pH2-3). Fractions were collected (0.5 ml to 1 ml) into 1.5 ml eppendorf

tubes (Sarstedt, Newton, NC). The samples were adjusted to a physiological pH by adding 100  $\mu$ l of the neutralization buffer (1.0 M TrisCl pH 8.0). The fractions with the highest optical density were pooled.

### **2.2.3 Production and Purification of Antibodies from Ascites Fluid**

Selected hybridomas were injected into pristane-primed 129x BALB/c OPN-deficient mice. The hybridomas generated ascites in the peritoneal cavity. The ascites fluid was generously tapped by Dr. Yacov Ron (Department of Molecular Genetics and Microbiology, RWJMS, UMDNJ). Ascites fluid was passed through a Nitex mesh to remove debris. After centrifugation at 5000 rpm for 12 min, the lipid layer in the ascites fluid was removed. While stirring on ice, saturated ammonium sulfate (SAS) was added drop wise until 58% saturation was achieved. After remaining on ice for 20 min and after subsequent centrifugation at 7000 rpm for 10 min, the pellet was drained by inversion. The pellet was dissolved in three times the original volume of the ascites fluid using 3.0 M NaCl/1.0 M glycine pH 8.0 loading buffer. The partially purified immunoglobulin was loaded onto a 50-ml column that was pre-packed with 12 ml of a 50% slurry of protein A. The column was equilibrated with 20 ml of loading buffer before adding the antibody preparation. After washing the column with 25 ml of loading buffer, the antibody was eluted with 50 ml of 0.1 M glycine/0.5 M NaCl pH2.5. Typically, the column was loaded, washed and eluted using a pump to deliver 2 ml fractions at 6-min intervals. During the elution, fractions were collected into tubes containing 250  $\mu$ l of 1.0 M TrisCl pH 8.0 to immediately neutralize the acidity. The fractions with the highest optical density were pooled, dialyzed against PBS and lyophilized. In later preparations we sought to adjust the antibody concentration to 1 mg/ml and lyophilize 1 mg aliquots.

## **2.3 Project 2: HUVEC Cell Culture and Apoptosis of Growth Factor-Deprived HUVEC Cells**

### **2.3.1. HUVEC Cell Culture and FACS Analysis**

Human umbilical vein endothelial cells (HUVECs) (American Type Culture Collection, ATCC) were continually cultured on 0.2% gelatin (porcine Type A, Sigma, St. Louis, MO) coated 10-cm or 6-well plates with Medium 199 (Invitrogen, Grand Island, NY) supplemented with 2mM L-glutamine, 100u/ml of penicillin, 100µg /ml streptomycin, 10% heat-inactivated fetal bovine serum (Hyclone, Logan, UT) for 30 min 58°C, heparin (5U/ml; Sigma), endothelial cell growth supplement (ECGS, 7.5µg/ml; Sigma), and  $\alpha$ FGF (4ng/ml; Sigma) [Khan et al., 2002]. Cells were maintained at 37°C in 5% CO<sub>2</sub> for at least 3 days until 80% confluency and were passaged by detaching with 0.05% trypsin-EDTA (Invitrogen, Grand Island, NY). Viability was determined by Trypan Blue exclusion and cells were counted with a hemocytometer.

Once cells were near confluency, Medium 199 and 1.0% bovine serum albumin (BSA, Sigma) was added in all cases when the HUVECs were deprived of added growth factors (serum, ECGS, heparin, L-glutamine, and  $\alpha$ FGF). OPN was added to growth factor-starved cells at 1:10 dilutions starting with 300 ng/ml down to 0.3 ng/ml. The positive control had the normal complete medium without added OPN and the negative control had neither growth factors nor OPN. The OPN used in this experiment was purified human milk OPN generously provided by Dr. E. Sørensen. After 24 to 48 hr in which controls were working properly, the cells were analyzed by flow cytometry analysis software (FACS) by Gary Ren in Professor Yufang Shi's laboratory.

## **2.4 Project 3: Culturing HS766T Pancreatic Cancer Cells**

The HS766T pancreatic cancer cells were provided by Dr. Hwyla Arafat (Thomas Jefferson University), the PI on the NIH grant that supported this project. They were cultured in complete medium that contained DMEM (Mediatech Inc., Herndon, VA) supplemented with 2mM L-glutamine, 100u/ml of penicillin, 100µg /ml streptomycin and 10% fetal bovine serum (FBS) (Hyclone, Logan, UT) in 10-cm plates. Cells were maintained at 37°C in 5% CO<sub>2</sub> for at least 2 days until 80% confluency and were passaged by detaching with 0.25% trypsin-EDTA (Invitrogen, Grand Island, NY).

### **2.4.1 Transfecting DH5α with plasmid 636i, OPN FL, OPN C**

The OPN FL and OPN C plasmids, used to over-express OPN, were generously provided by Dr. Xin Wang (NIH). These plasmids consist of SV40 promoter/enhancer to drive replication in mammalian cells, a gene encoding ampicillin resistance, and the constitutively active cytomegalovirus (CMV) promoter. Since the cells were already making OPN this could mask a small increase in OPN expression. The plasmid 636i, used to downregulate OPN expression, was kindly provided by Dr. Lalita Samant-Shevde of Mitchell Cancer Institute. This plasmid, derived from pSuper vector (OligoEngine, Seattle, WA), was engineered to produce an siRNA targeting OPN [Shevde et al., 2006]. *E. coli* DH5α cells were transfected by Tanya Gordonov with plasmid 636i to generate working amounts of the plasmid DNA.

### **2.4.2 Transfecting HS766T cells**

Cells from a 10-cm plate were equally distributed in a 6-well plate. Once the cells reached confluence, they were transfected as per the manufacturer's instructions. The transfection mixture contained DNA, complete medium for HS766T cells, and Transfast

(Promega, Madison, WI) transfection reagent. The reagents were combined, vortexed and incubated at room temperature for 15 min. The complete medium was removed from the 6-well plates and 1 ml of the transfection mixture was added to each well. The cells were then incubated at 37°C in 5% CO<sub>2</sub> for 1 h. Afterwards, 2 ml of complete medium was added to each well to bring the final volume to 3 ml. The DNA used here was from the plasmid 636i, the OPN full-length (FL) plasmid, or the OPNc plasmid, which is a splice variant of OPN FL.

#### **2.4.3 Selection of Stably Transfected HS766T Cells**

Stable transfection selection was performed 24 to 48 hr after transfection. The complete medium in the 6-well plate was removed and the cells washed 3 times with PBS; 300 µl of 0.25% trypsin EDTA was added to each well for 4 min. Complete medium was added to each well to stop the trypsinization. The cells were centrifuged and the supernatant discarded. The cells were resuspended in 1 ml of complete medium for each well and 30 µl of the resuspension was added to a new well in a 6-well plate that contained the appropriate selective medium. Each well in the 6-well plate had 30 µl of resuspension from its respective tube. Cells transfected with the 636i plasmid were treated with a selective medium containing puromycin at a concentration of 0.1 µg/ml or 0.05 µg/ml. Cells transfected with the OPN FL and OPN C were treated with neomycin at a concentration of 400 µg/ml or 600 µg/ml. The amount of drug used varied slightly and had to be optimized by doing a kill curve.

#### **2.4.4 Colony Selection and Cloning of HS766T cells**

When large independent colonies could be seen with the naked eye, they were marked for selection. A sterile cloning ring was dipped in sterile silicone gel and the ring

then placed around the center of the colony. The medium was removed from the inside of the cloning ring, washed with PBS 3 times and 100  $\mu$ l of 0.25% trypsin-EDTA was added. The cells were removed from inside of the cloning ring once they were detached and were placed into one well of a 6-well plate with 2 ml of DMEM. The individual colonies were maintained until 90% confluence and then were passaged with 0.25% trypsin-EDTA to a 10-cm plate. Once the 10-cm plate reached confluency, it was split into two 10-cm plates. After both plates of an individual colony were confluent, cells from one plate were frozen down; RNA was extracted from cells in the other plate.

#### **2.4.5 RNA Extraction of HS766T Clones**

HS766T total cellular RNA was extracted by the Trizol method as per the manufacturer's instructions. Trizol (Invitrogen, Grand Island, NY) was used to lyse the cells from the 10-cm plate. Chloroform was added to the lysate to separate the red phenol-chloroform phase from the aqueous phase in which the RNA remained. The aqueous phase was mixed with 100% isopropanol to precipitate the RNA and then the RNA was washed with 75% ethanol. The RNA pellet was dried under a vacuum and resuspended in diethyl pyrocarbonate (DEPC)-treated distilled water. The RNA was then placed in a water bath for 15 min at 55 °C to facilitate the RNA dissolving and then the optical density was taken. A 260/280 ratio of 1.8 or greater was ideal.

#### **2.4.6 Reverse Transcription of HS766T RNA to cDNA**

The M-MLV reverse transcriptase kit (Invitrogen, Carlsbad, CA) was used and the recipe was optimized based on manufacturer's instructions. Each reaction when RNA was converted to cDNA contained 2  $\mu$ l of 50  $\mu$ M N6 random hexamers, 4  $\mu$ l of RNA sample (5  $\mu$ g), 4  $\mu$ l of dNTP (2.5 mM) and 10  $\mu$ l of sterile water. The thermocycler was

programmed to heat the samples at 65 ° C for 5 min and then the samples were quenched on ice for 3 min. Four µl of 5x first strand buffer and 2 µl of 0.1M DTT was added to each sample. The program was resumed at 25 ° C for 10 min then paused to add 1 µl of the M-MLV reverse transcriptase. The samples were incubated at 37 ° C for 50 min then inactivated at 70 ° C for 15 min. The samples were then run on a gel with a negative “no- RT” control, which had everything but reverse transcriptase.

#### **2.4.7 Semi-Quantitative PCR and Real Time PCR (qPCR) of HS766T cDNA**

Semi-quantitative PCR was done in order to determine which samples were going to be analyzed by real time PCR. Promega 5x Green GoTaq Reaction buffer (Madison, WI) was used for semi-quantitative PCR. Directions used were as per the manufacturer’s instructions. Each reaction consisted of 5 µl 5x Green GoTaq Reaction buffer, 2 µl dNTP mix, 2 µl 5 µM primer mix, 9.8 µl dH<sub>2</sub>O, 13 µl Platinum Taq DNA Polymerase (Invitrogen, Carlsbad, CA), cDNA 6 µl (50ng/µl). The thermocycler program was 95 ° C for 2 min, and 30 cycles at 95 ° C for 15 sec, 54 ° C for 20 sec, 72 ° C for 20 sec, and then terminated at 70 ° C for 15 min. Roche FastStart SYBR Green Master mix (Indianapolis, IN) was used for real time PCR analysis. Directions used were as per manufacturer’s instructions. Each reaction consisted of 5 µl of cDNA (250 ng), and 25 µl FastStart mix, 17 µl of dH<sub>2</sub>O and 3 µl of primer mix (600 nM in final reaction). The sequences of the human OPN primers are forward 5’ GCTTGGTTGTCAGCAGCA 3’ and reverse 5’ TGCAATTCTCATGGTAGTGAGTTT 3’ (Roche, Indianapolis, IN). The sequence of the human GAPDH (Glyceraldehyde 3-phosphate dehydrogenase) primers are forward 5’ GTATGACAACAGCCTCAA 3’ and reverse 5’ TCCTTCCACGATACCAAA 3’ (IDT, Coralville, IA).



For qPCR of each RNA sample, the cDNA was tested in triplicate. Each sample had two water controls in which 5  $\mu$ l water was added in place of the cDNA. The software used for the q PCR was SDS 2.0. The program was hold at 95 ° C for 10 min (Activates FastStart Taq DNA Polymerase) and the cycling was 95 ° C for 15 sec, 55 ° C for 60 sec for human OPN primer (GAPDH primer 50 ° C for 60 sec), and 72 ° C for 60 sec. The DNA Core Facility at UMDNJ ran the samples for me.

#### **2.4.8 Cell Migration Assay of HS766T Clones**

Based on the Real-Time PCR results, clones that showed the desired down-regulation or up-regulation of OPN were selected for the cell migration assay (wounding assay). A confluent monolayer of cells was washed 3 times with PBS then 2 ml of complete medium with 0.1% FBS was added. Each well was scraped with a 1-ml pipette tip one time in a horizontal plane in order to remove the cells. Nicotine was added at a concentration of  $3 \times 10^{-9}$ - $3 \times 10^{-7}$   $\mu$ M. The negative control had complete medium with 0.1% FBS and no nicotine and the positive control had complete medium with 10% FBS and no nicotine. Pictures were taken at 24 hr and 48 hr. Tonya Gordonov and I worked together on this assay. She used ASPC-1 cells instead of HS766T cells and I have presented both of our results in the results chapter.

## **Chapter 3**

### **Results**

#### **3.1 Project 1: OPN and Characterization of anti-OPN Monoclonal Antibodies**

##### **3.1.1 Background:**

In order to further characterize OPN and Anti-OPN mAbs, one of my projects was to purify OPN and selected mAbs and then characterize them by gel electrophoresis and ELISA. The mAbs were either made by growing hybridomas then concentrating and purifying the conditioned medium or by growing cells as ascites. Dr. Yacov Ron performed all injections in the mice and removed the ascites from the mice. From there I purified the antibody.

##### **3.1.2 Strategy:**

###### **3.1.2.1 OPN Characterization**

OPN purification was previously done by binding OPN to the 2A1 monoclonal antibody coupled to protein G beads [Kazanecki, 2007]. This method often did not produce as high of a yield as desired. Therefore, we switched to DEAE ion-exchange chromatography. The serum-free conditioned medium was obtained from ras-transformed 275-3-2 fibroblasts [Wu et al., 2000]. Conditioned medium was added to the column containing DEAE in the low salt wash buffer that allowed the OPN to bind to the DEAE. OPN was eluted from the DEAE as the salt concentration was increased. A SDS-PAGE gel was run in order to determine which samples had the highest amount of OPN. Previously, a silver-stain was used to determine this, but so much OPN was present that it could be seen with Coomassie Blue stain. Figure 4 shows what a typical gel of one of the OPN preparations. A quarter of the way through the elution is where the

majority of the OPN eluted; phenol red came off somewhat later. Figure 3 shows the conductivity of a typical OPN purification. The majority of the OPN was eluted around 250 $\mu$ S to 350 $\mu$ S. The phenol red eluted around 630 $\mu$ S to 730 $\mu$ S. Fractions containing OPN were desalted, dialyzed against PBS, and lyophilized. This OPN was used in several of my experiments as well as other lab experiments.

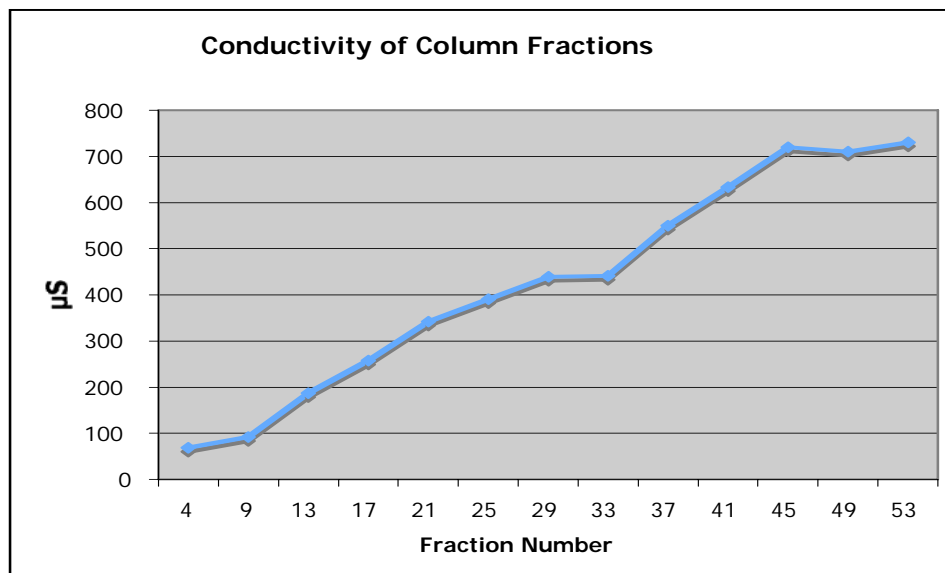


**Figure 3. Conductivity of OPN Fractions.** The majority of OPN eluted around 250 $\mu$ S to 350 $\mu$ S and the phenol red at 630  $\mu$ S to 730  $\mu$ S. Phenol red is a pH indicator. Conductivity was measured as a dilution of 100  $\mu$ l of OPN in 900  $\mu$ l in dH<sub>2</sub>O.

### SDS-PAGE Analysis of OPN Preparation

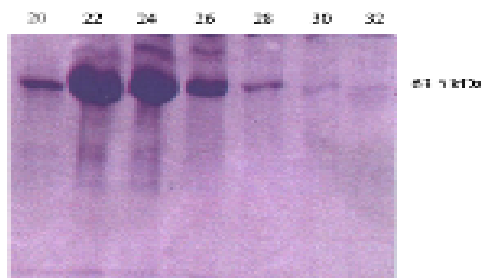


**Figure 4. Analysis of Fractions Where OPN Eluted.** OPN can be found around 65-75kDa. Every other fraction was analyzed. Samples 20-24 would be pooled, desalted, dialyzed and then lyophilized.

#### 3.1.2.2 Characterization of anti-OPN Monoclonal Antibodies

Hybridoma conditioned medium was obtained by growing cells in SFHM for 1-2 weeks, filter sterilizing and then concentrating by use of Centriprep YM-10. The concentrated medium was then purified using immobilized protein G, A, or A/G. It was determined by trial and error which immobilized protein worked best for each antibody since each antibody has a different specificity for the immobilized protein. Lastly, it was desalted and the fractions with the largest amount of antibody were pooled.

The mAbs derived from ascites were purified by ammonium sulfate precipitation and DEAE-Sepharose column chromatography. Fractions containing the majority of the  $A_{280}$  were pooled, dialyzed against PBS, and lyophilized. The mAbs made from ascites and conditioned media were characterized by both ELISA and SDS page analysis. Figure 5 shows an SDS-PAGE gel stained by Coomassie Blue of several of the antibodies concentrated from conditioned medium. Heavy and light chains are visible in 1H3F7 and 39F10. The heavy chain is visible in 21F12 and 8A7. The light chains are weak in these antibodies. Lastly, 7B4 shows weakly the heavy and light chain. The largest upper band in all of the samples is transferrin. All of the antibodies appear to be IgGs.

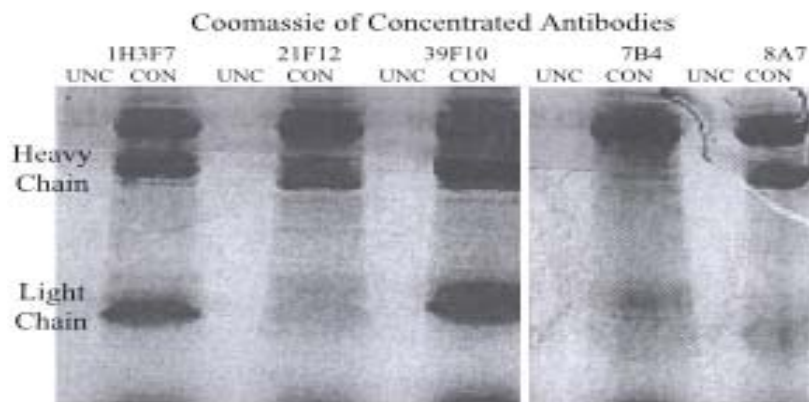


**Figure 5. Monoclonal Antibodies Purified from Conditioned Media.** Heavy and light chains are visible in 1H3F7 and 39F10. 21F12 and 8A7 show the heavy chain and little to no lower chain. 7B4 shows very little heavy or light chains. All of the preparations show a slower-migrating species (MW~75-85kDa), which is transferrin, present in the SFHM. UNC are the unconcentrated medium; the concentrated samples (~50x) are labeled as CON.

Figure 6 shows SDS-PAGE gels of antibodies that were purified from ascites generated from hybridomas. (Hybridomas producing 2A1, 2C5, 2D6, 1H3F7, 1G4, and 10H4cl5 were cloned). Most of the monoclonal antibodies purified from the ascites preparations appear to be fairly pure IgGs. The heavy chain of an IgG is around 50-55kDa. There are a few antibodies that were purified from ascites that do have an even larger upper band than the heavy chain, such as 65D2, 42B12, and 67F7. Most of the antibodies purified by ascites did not have this larger upper band. This larger band may be covalently linked heavy and light chain or the  $\mu$  chain of IgM. In order to test this, a western blot was done where a goat polyclonal to mouse IgM that is specific for the  $\mu$  chain and is conjugated to HRP (Abcam, Cambridge, MA) was used. Results can be seen in Figure 7. The positive control used was IgM and the band can be seen and there was a band at the same size as the control. Therefore, 67F7 made from ascites is an IgM.

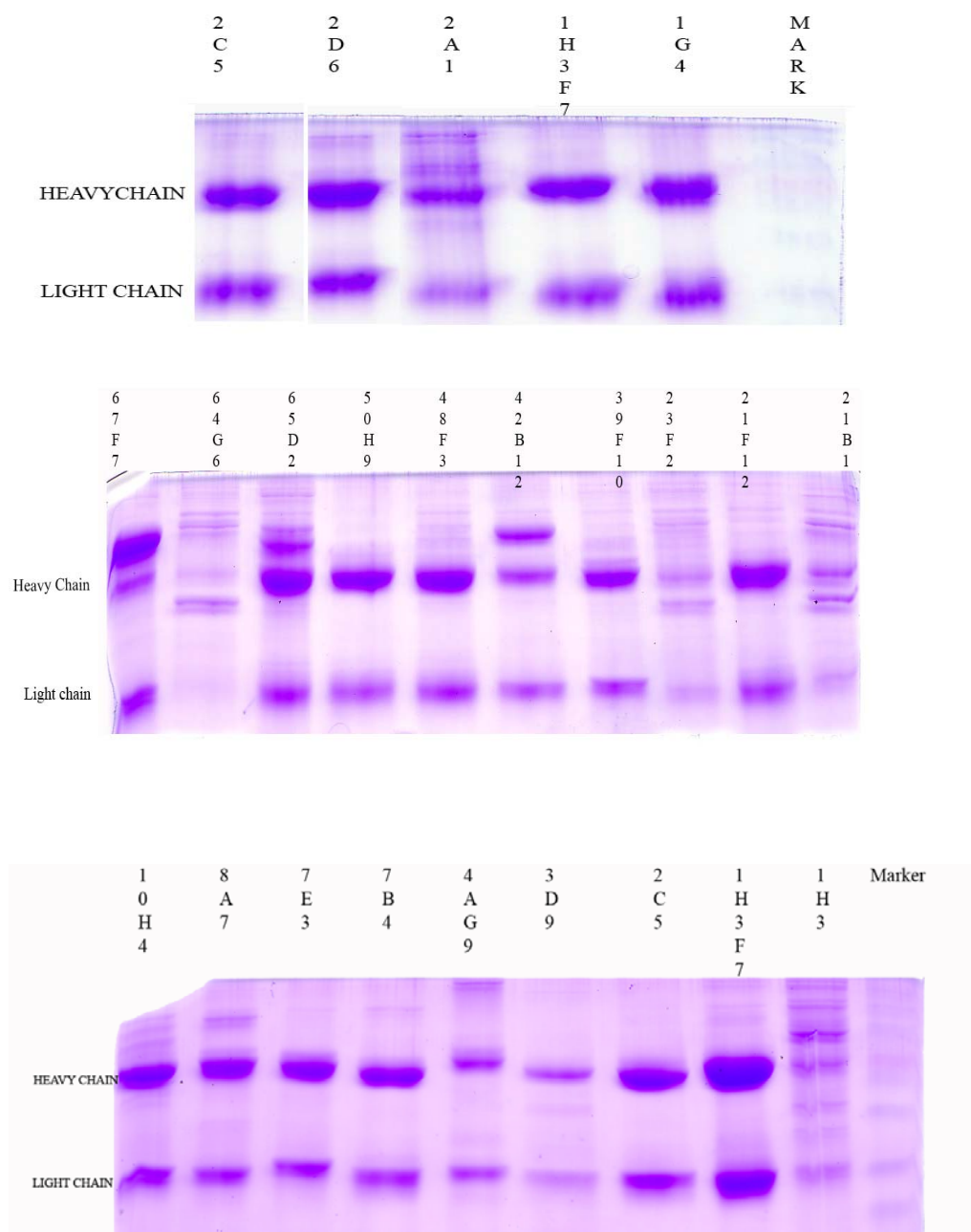


**Figure 6. SDS PAGE Coomassie Blue Stained Gel of Antibodies Purified from Ascites.** Heavy and light chains are clearly visible. The heavy chain is around 55 kDa and the light chains around 25kDa. All antibodies but 2A1 are very clean. The bands above the heavy chain in 2A1 may be cross linked species. A second independent preparation of 2A1 did not have as much of this material. Courtesy of Cassandra Louis.

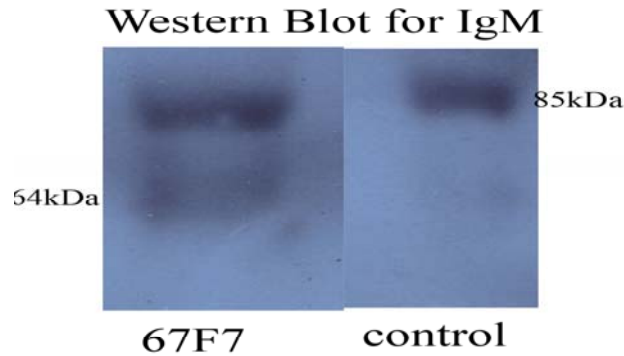


**Figure 7. Western Blot to Determine if an IgM is Produced by 67F7.** The control IgM band can be seen at 85kDa and there is a band at 85kDa in the lane 67F7. This was developed for 10min and was blocked overnight with 4% nonfat milk. Others tested were negative (42B12, 65D2). The smaller band in 67F7 has not been determined.

The ELISA results were not consistent in terms of the Coomassie Blue results (Figure 8). This is to be expected since the affinity of each antibody for OPN varies.

2A1 is one of the best antibodies that have been made in our lab. It binds strongly to both human native OPN (hnOPN) and human recombinant OPN (hrOPN). This antibody was often used as a control because it binds strongly to OPN and is very reproducible.

10H4cl5 is also another antibody that recognizes hnOPN and hrOPN. It does not recognize it as well as 2A1. All of the information from the antibodies made from conditioned medium or ascites has been catalogued in our database so that we can retrieve results from Elisas, Westerns, Coomassie Blues, and Peptide assays.

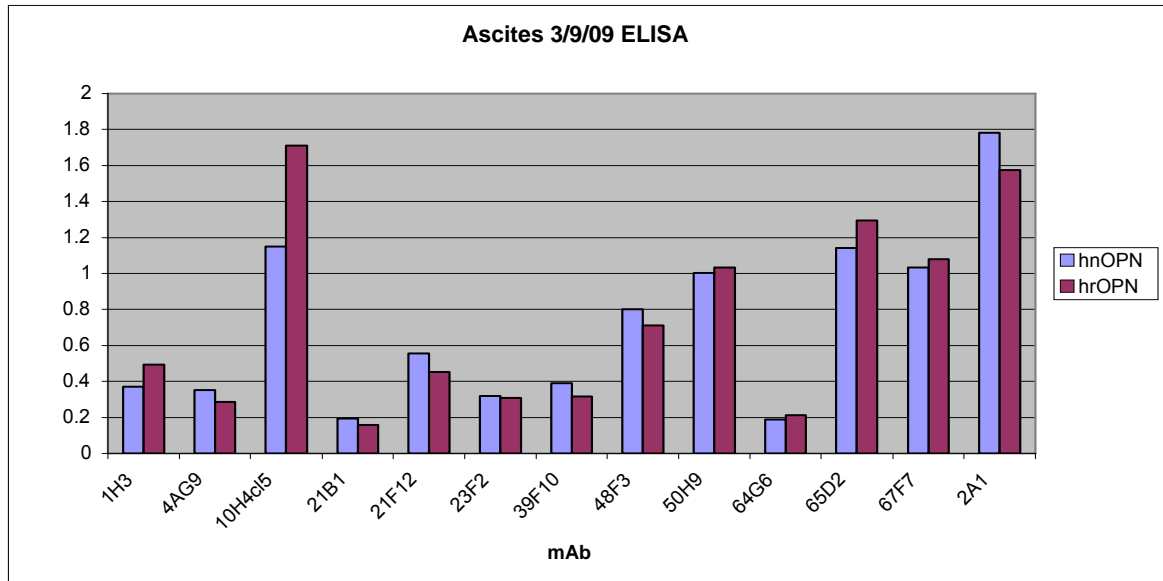


**Figure 8. Elisa on mAbs Made from Ascites Fluid.** Human native OPN and human recombinant OPN were used as the antigen. Each mAb has a different efficiency for OPN. 2A1 has a very high affinity for hnOPN and hrOPN. Results with a 0.3 OD or less and a poor Coomassie staining were considered to be weak antibodies. Courtesy of Cassandra Louis.

### 3.2 Project 2: HUVEC Cell Survival

#### 3.2.1 Background:

It was previously shown that soluble OPN could protect human umbilical vein endothelial cells (HUVECs) from undergoing apoptosis when the cells were deficient in critical growth factors and cytokines [Khan et al., 2002]. OPN was able to suppress apoptosis and repress DNA fragmentation in a dose-dependent manner. It was proposed that one of the functions of OPN with endothelial cells was to save stressed cells by preventing them from going through apoptosis. It was hypothesized that this was due to OPN occupying unligated receptors.

#### 3.2.2 Hypothesis:

We hypothesized that since OPN could protect endothelial cells from going through apoptosis that certain mAbs could inhibit the action of OPN and therefore



suppress the protection that OPN otherwise provides to growth factor-deprived endothelial cells.

### **3.2.3 Strategy:**

HUVEC cells were grown to about 80% confluency in a 6-well plate. Complete conditioned medium was removed from the wells. The cells were then starved with 2 ml of Medium 199/1% BSA in addition to OPN. The amounts of OPN added to the growth factor-starved cells were 300ng/ml, 30ng/ml, 3ng/ml and 0.3ng/ml. There were also two control wells. One well had the normal complete medium without added OPN and the other control had neither growth factors nor OPN. After 24 hr, the results were determined by FACS analysis. After several attempts, we were successful at demonstrating protection of OPN on endothelial cells. The experiment worked a few times but only one time did it work well enough that you could visually see the difference in the wells. However, since our results were not reproducible, we did not test the effect of mAbs on OPN protection in endothelial cells. The experiment that yielded the best results is shown below in Figure 9. Our inability to obtain reproducible results has been frustrating, likely due to variability in cell physiology.

Cell culture pictures show that the two controls gave the expected results. In control number 1 we expected the cells to grow without a problem since all cytokines and growth factors were present. Control 2 showed a lot of cell death due to the lack of growth factors. Wells 3-6 showed that OPN is protecting cells from apoptosis since more of the cells have survived in comparison to control number 2. The cells also look visually healthier in comparison to control number 2. This can be seen by the extensions that are present in the healthier cells and not present in the apoptotic cells.

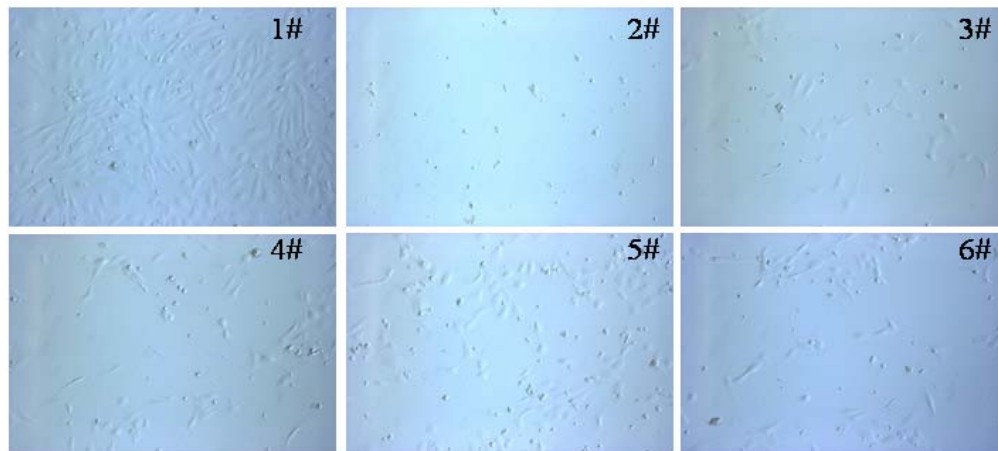


**Figure 9. FACS Results of HUVEC Cells in Apoptosis.** Control 1 shows healthy cells and control 2 shows apoptotic cells. Wells 3-6 show an increased number of cells surviving due to protection from OPN. Courtesy of Gary Ren.

Figure 10 shows a FACS analysis of the HUVECs. The M1 population in well number 1 was very low as expected since this number suggests that there are few apoptotic bodies. When comparing this to well number 2, the M1 population is very high as expected since these cells were deprived of growth. The peak in each graph represents the number of diploid G1 cells. As expected, the peak in well number 1 is larger than well number 2 since these cells were not deprived of growth factors. The M2 population represents the number of dividing cells present (S+G2). The M2 number of well 2 is very low because very little cell proliferation is occurring and many of the cells have undergone apoptosis. Comparison of wells 3-6 reveals the protective effect of OPN by the increase in the fraction of cells in M2.

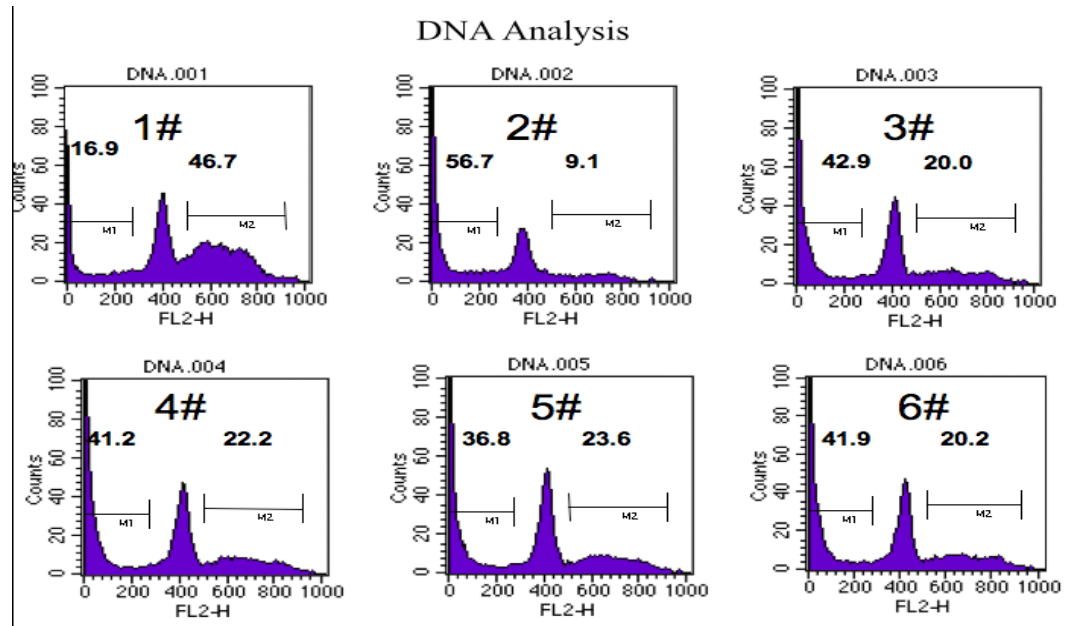
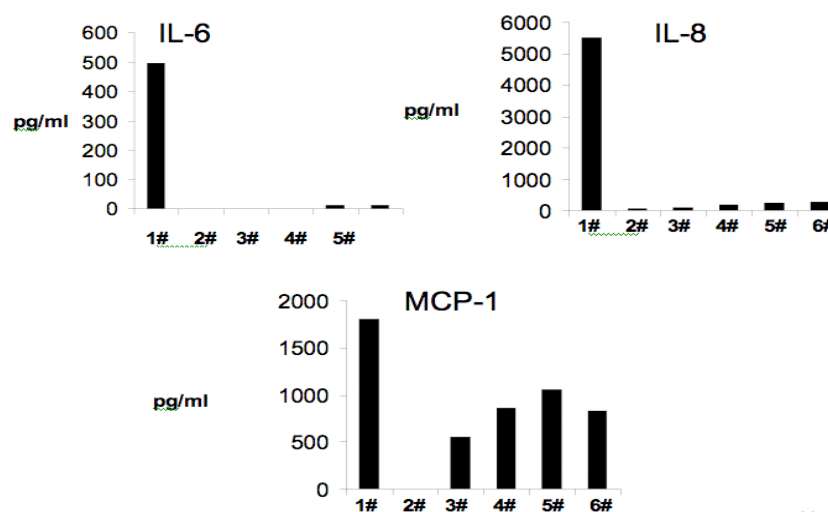


**Figure 10. DNA Content Analysis.** M1 is largely composed of apoptotic fragments. M2 indicates how many cells are proliferating. The peak represents how many diploid G1 complete cells are present. The cells are healthy in control 1 and in control 2 the cells are going through apoptosis. Wells 3-6 show that OPN is protecting some of the cells from apoptosis. Courtesy of Gary Ren.

In Figure 11, the cytokine assay shows that OPN does not have any effect on Interleukin-6 or Interleukin-8 production. However, monocyte chemoattractant protein 1 (MCP-1) production is enhanced within a range of OPN concentrations.

## Cytokine Assay

pg/ml	IL-6	IL-8	MCP-1
1#	495.46	5503.94	1803.07
2#	0	73.37	0
3#	0	98.4	556.17
4#	0	182.85	864.3
5#	11.89	243.42	1058.28
6#	13.19	262.29	826.93



11

**Figure 11. Cytokine Assay of HUVEC Cells.** OPN does not effect IL-8 or IL-6 production. MCP-1 levels are elevated at low concentrations of OPN. Results provided by Guangwen (Gary) Ren.

### 3.3 Project 3: Nicotine Induces OPN in Pancreatic Ductal Adenocarcinoma Cells

#### 3.3.1 Background:

This project is a collaboration with a lab at Thomas Jefferson University under Dr. Hwyla Arafat. Our lab was to conduct a part of the NIH-supported research that involved examining the action of nicotine on various properties of pancreatic ductal adenocarcinoma (PDA) cells expressing different levels of OPN. Previous research

conducted in Dr. Arafat's lab showed that OPN expression is induced by nicotine and cigarette smoke in the pancreas and PDA cell (Chipitsyna et al., In press, 2009). They determined that this is achieved through activation of the OPN promoter. They were able to show that nicotine contributes to PDA pathogenesis through up-regulation of OPN. Our part in this collaboration was to study the involvement of OPN in the survival, proliferation, migration, and invasion of the PDA cells in vitro.

In order to verify that OPN does affect the metastatic phenotype, PDA cells were permanently transfected with vectors design to increase or decrease endogenous OPN expression. Once this was accomplished the intent was to assess the proliferative, migratory, and invasive capabilities of the cells in various concentrations of nicotine in cell culture.

### **3.3.1 Hypothesis:**

In pancreatic cancer, we hypothesize that OPN would affect the nicotine-induced changes in cell proliferation, invasion, survival and migration in vitro.

### **3.3.2 Strategy:**

HS766T cells were permanently transfected with either the siRNA plasmid 636 to down-regulate OPN or plasmids to overexpress OPN: OPN-C (a splice variant of OPN) and OPN-FL, full-length OPN. The cells were transfected with Transfast (Promega, Madison, WI), a cationic liposome reagent. After stable transfection with puromycin (for down-regulated cells) or neomycin (for up-regulated cells), clones were selected and grown out. RNA was extracted from each clone and then cDNA made by reverse transcription. A semi-quantitative PCR was performed afterwards followed by qPCR analysis.

Semi-quantitative PCR was performed on all clones and based on the results certain clones were selected for Real-Time qPCR analysis. The GAPDH primer, a house-keeping gene, was used to normalize the data. Figure 12 shows all clones tested with GAPDH primer. The length of the expected GAPDH amplicon is 127 bp. Clone C-7 and clone 636-F do not show a band likely because the cDNA is bad. The negative control as expected does not show a band. All of the other clones consistently showed a band around 127bp.

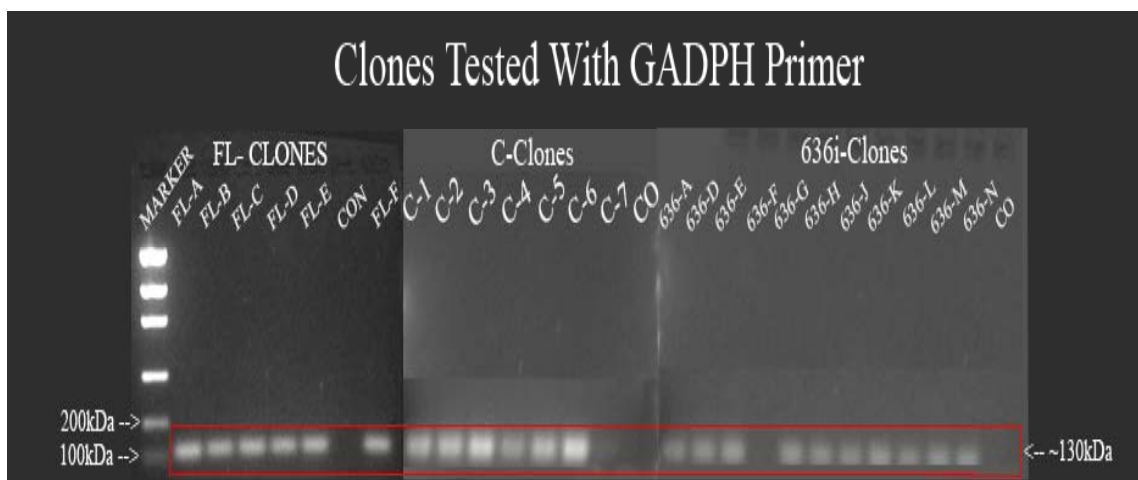


**Figure 12. Relation of mRNA Levels Tested with House Keeping Gene.** Bands are visible around 130bp. Negative controls do not show a band. Clones C-7 and 636-F do not show a band because the DNA is not good. The bands within each PCR generate a fairly consistent visual intensity of the band. Full length clones are designated by “FL” followed by a number and OPNc clones are designated by “C” and then a number, and down-regulated clones by “636” followed by a letter.

The OPN primer was designed using the ROCHE primer design program. Figure 13 shows the clones tested with the OPN primer. The down-regulated 636 clones show a band around 130 bp. This is the expected size of the amplicon. All down-regulated clones (indicated by “636-Letter”) worked except 636-F. Also clone C-7 which is supposed to up-regulate OPN expression did not work. This matches the previous results with GAPDH. This suggests that the cDNA of these clones are not good. The intensity

of the bands from the down-regulated clones when compared to the parent, show that they are apparently down-regulating in the amount of OPN being expressed. Clone E (636) seems to have the same intensity as the parent and therefore may not be a good candidate for Real Time Analysis. All PCRs, except for the OPN-FL clones were run with the same amount of cDNA.

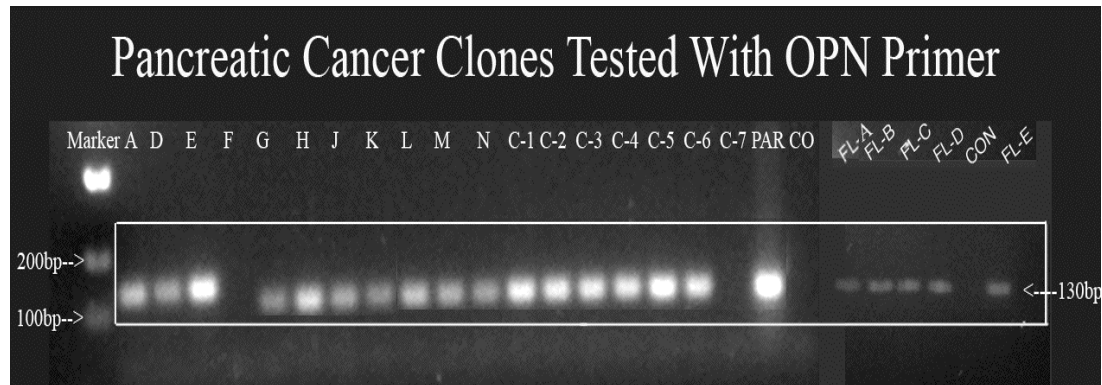


**Figure 13. Relation of mRNA Levels Tested with OPN Primer.** Bands are visible around 130bp. Negative controls do not show a band. Clones C-7 and 636-F do not show a band because the DNA is not good. Full length clones are designated by “FL” followed by a number and OPNc clones are designated by “C” and then a number, and down-regulated clones by just a capital letter.

Some of the OPN-C clones (designated by letter “C” then a number) and the OPN-FL clones (designated by “FL” followed by a letter) appear to have been up-regulated compared to the parent. A band around 130 bp can be seen. The expected amplicon size is 130bp. The negative controls do not have a band as expected. This PCR analysis of the clones suggested which clones would be the best to test in the Real-Time qPCR analysis. HS766T cells produce endogenous OPN and therefore the amount of OPN that the cells have can be used as a reference to what is significant in term of clones that up-regulate OPN.

Figure 14 shows an SDS-PAGE gel stained by Coomassie Blue of the parent cell-conditioned medium. A visible band appears around 70 kDa. This confirms that the parent cells are indeed making a high amount of extracellular OPN.

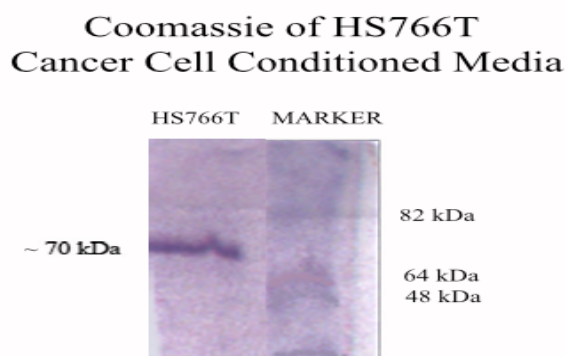


**Figure 14. SDS-PAGE Analysis of the Parent Cell Serum-Free Conditioned Medium.** A visible band appears around 70 kDa. This shows that the parent cells are making a high amount of extracellular OPN.

In Figures 15 and 16, amplification plots using the GAPDH primer and Roche OPN primers are shown. The results are displayed as a sigmoid curve on a logarithmic scale. When converting the information from the logarithmic scale, it reveals a straight-line relationship between the amount of DNA and the cycle number. Cycle 15 is where amplification starts in the GAPDH samples and cycle 15 is where amplification starts in Roche OPN samples. GAPDH samples plateau at 27 cycles and Roche OPN samples at 35 cycles. In each plot, the water controls are to the far right and even though there is amplification it is many cycles later. This is artifact and is very common in qPCR. These graphs indicate fluorescence on the y-axis and cycle number along the x-axis. The red line indicates the threshold as which Ct values are given.



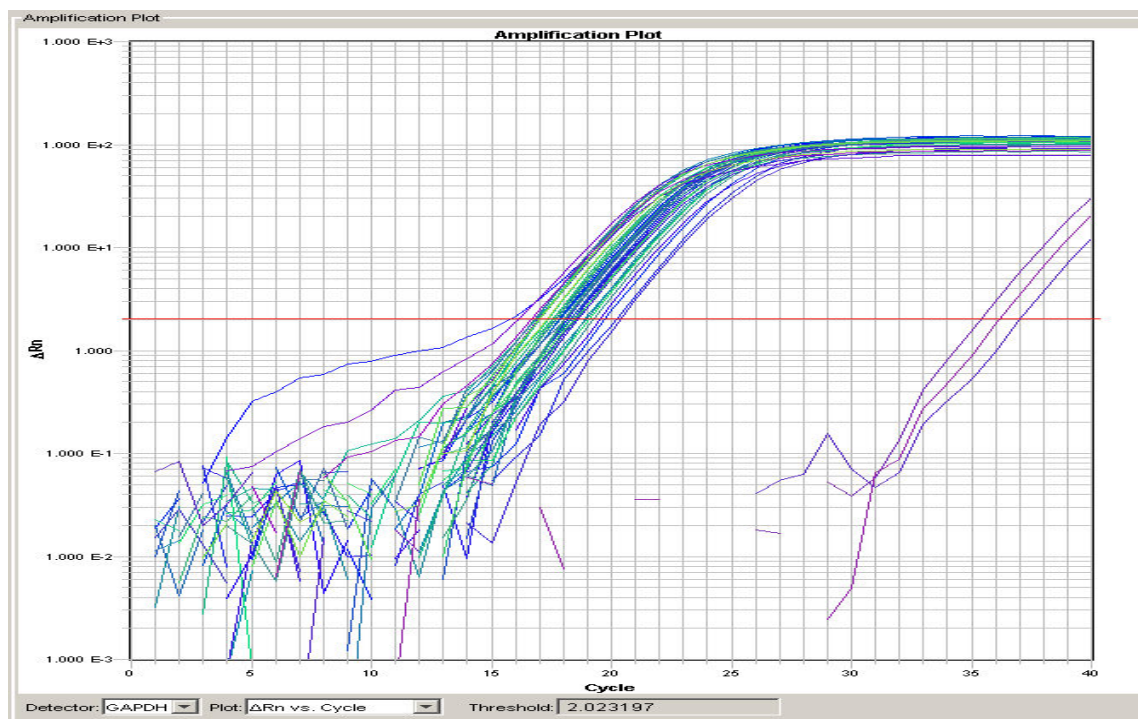


**Figure 15. GAPDH Control Amplification Plot.** Around cycle 15 is where amplification started. The water controls are on the far right. This is expected since there was no DNA and the amplification, if any, is late in the cycles. Each clone was done in triplicate and the average values were taken. Around cycle 27 is where the amplification plateaus.

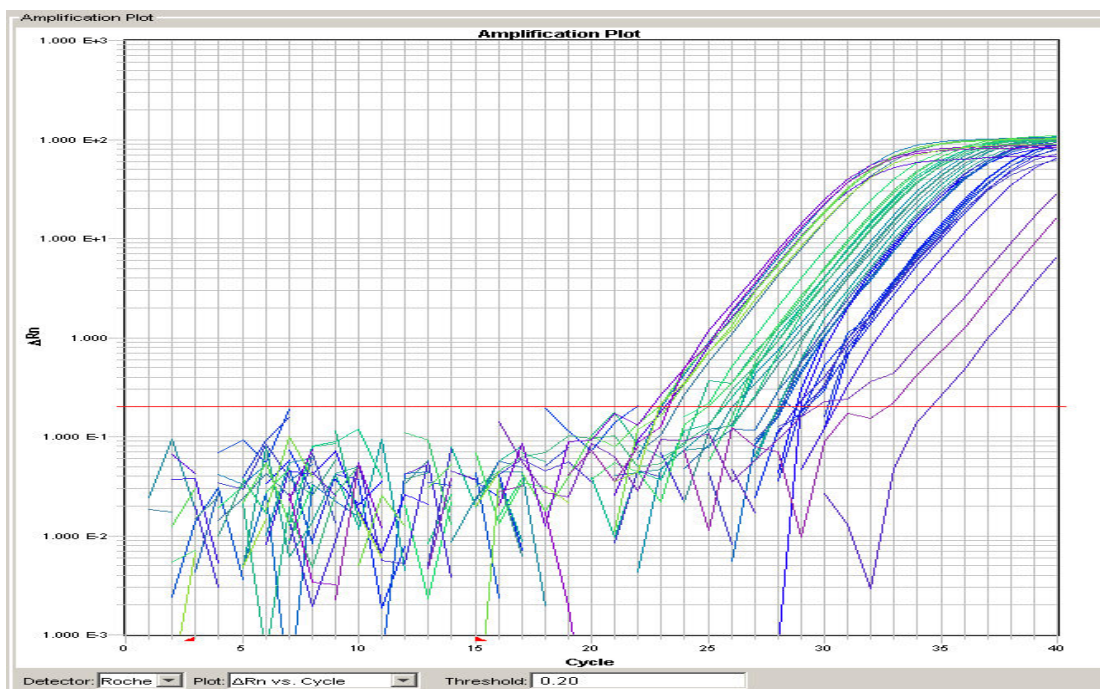


**Figure 16. Roche OPN Primer Amplification Plot.** Around cycle 25 is where amplification started. The water controls are on the far right. This is expected since there was no DNA and the amplification, if any, is late in the cycles. Each clone was done in triplicate and the average values were taken. Around cycle 35 is where the amplification plateaus.

In Figures 17 and 18, the dissociation (melt) plots from the qPCR are shown.

Both peaks have a consistent dissociation temperature, which suggests that they are a homogeneous in terms of the sequence that was amplified. The dissociation temperature of GAPDH product was 79°C and 85.5°C for the Roche OPN primer product.

### GAPDH Control Dissociation Curve

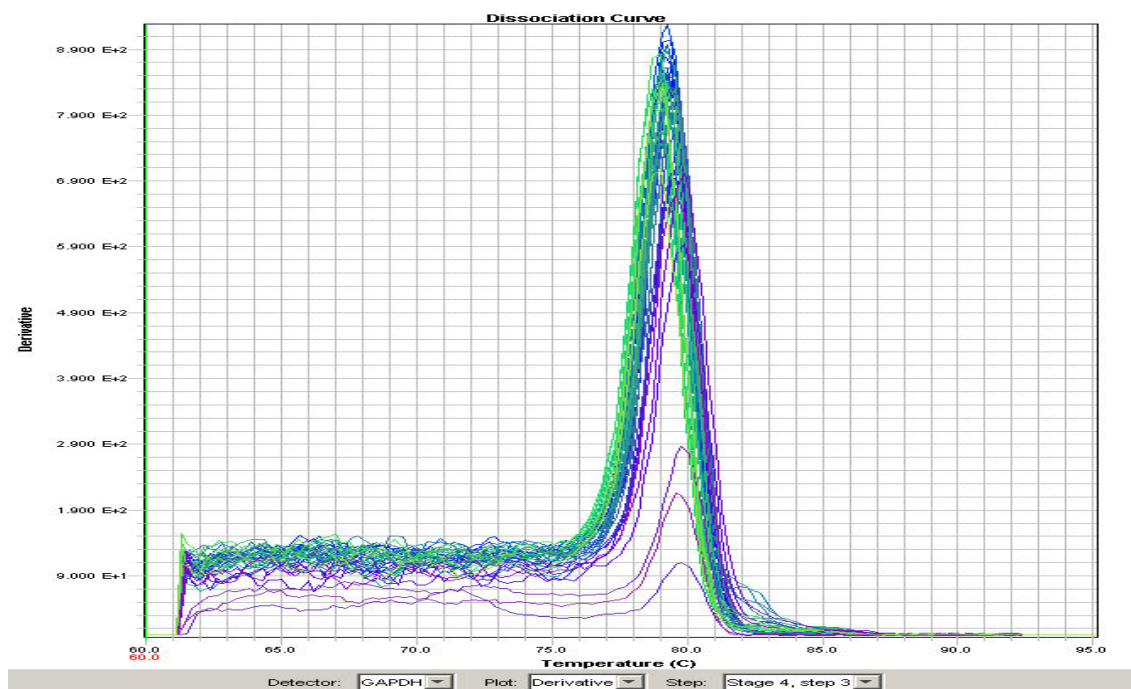


**Figure 17. GAPDH Control – Dissociation (Melt) Curve.** The melt of the homogeneous population is at 79°C. This shows that the primers consistently amplified the same region. The small low peaks are the water controls, which since they came up several cycles later are artifact.

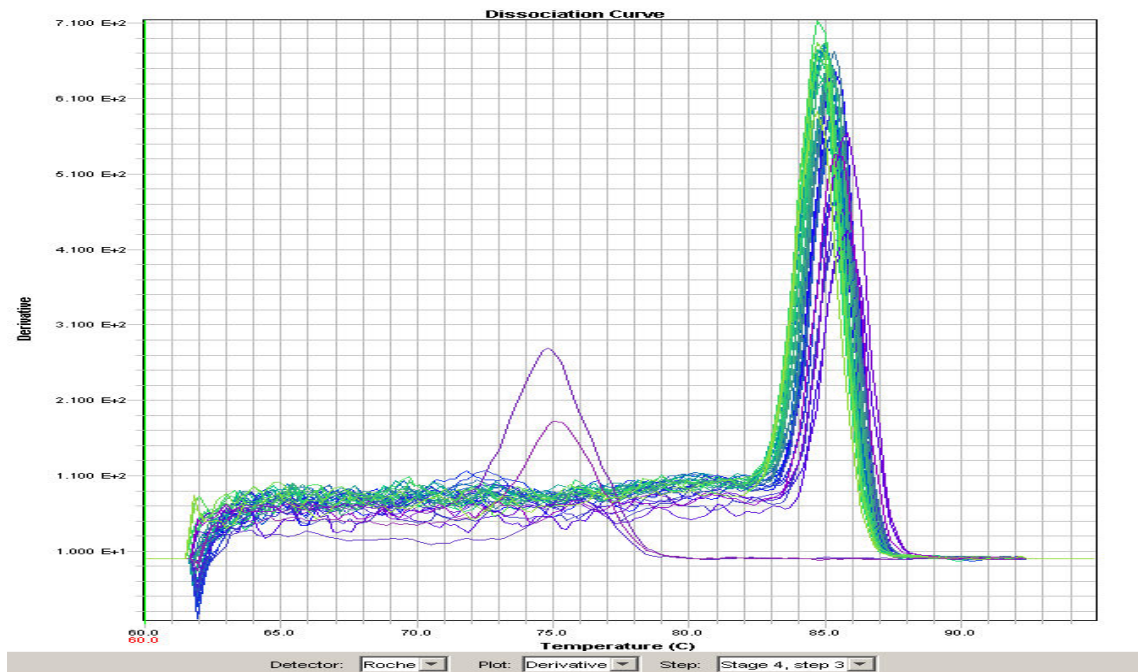


**Figure 18. Roche OPN Primer – Dissociation (Melt) Curve.** The melt of the homogeneous population is at 85.5°C. This shows that the primer consistently amplified the same region. The small low peaks to the left are the water controls, which since they came up several cycles later are an artifact.

### 3.3.3 PCR Calculations

The formula,  $2^{-\Delta\Delta C_t}$ , is used to determine relative changes in gene expression from qPCR experiments. Based on this formula, I calculated the fold difference or relative changes in gene expression when compared to the parent clone and the housekeeping gene [Luo, Honors Thesis, 2008] For the equations below, “Time X” indicates any time point and “Time 0” indicates the time that 1x expression of the target gene is normalized to the housekeeping gene. All samples were done in triplicate and the  $C_t$  values were averaged. In equation 2, the average  $C_t$  values of the housekeeping gene were subtracted from the values of the averaged  $C_t$  values from the test gene during a variable condition by “Time X”. In equation 3, the average  $C_t$  values of the housekeeping gene were subtracted from the values of the averaged  $C_t$  values from the

test gene during the initial condition by “Time 0”. Lastly, equation 4 is used to calculate the fold change. Results from equation 2 and 3 are subtracted to give a value to equation 1. This then gives the overall  $\Delta\Delta CT$  value. Next, product of equation 1 is inserted into equation 4 to give to give the fold difference value. Fold change value gives a more accurate assessment of the gene expression results because the Ct values are normalized with the housekeeping gene.

### **Equation 1: Normalizing Gene Results**

$$\Delta\Delta CT = (C_{T, \text{Target}} - C_{T, \text{Housekeeping Gene}})_{\text{Time x}} - (C_{T, \text{Target}} - C_{T, \text{Housekeeping Gene}})_{\text{Time 0}}$$

### **Equation 2:**

$$(C_{T, \text{Target}} - C_{T, \text{Housekeeping Gene}})_{\text{Time x}}$$

### **Equation 3:**

$$(C_{T, \text{Target}} - C_{T, \text{Housekeeping Gene}})_{\text{Time 0}}$$

### **Equation 4: Calculation of Fold Difference**

$$2^{-\Delta\Delta Ct}$$

The Tables 1 and 2 below shows the application of equations 1-4. These samples are of the clones tested with GAPDH primers and Roche OPN primers. The results will then be compared to the untransfected parent cells. Several of the down-regulating clones worked but only the best are shown below in Table 1. Ideally we would like to see a fold value of 4 to be considered to be significant in terms of over-expression of OPN. Clone FL-G gave a fold value of 1.23. Technically anything over a fold value 1 of is considered to be up-regulating while anything below 1 is down-regulating. Clone FL-G fold value of 1.23 means that there is 1.23 times more template which may not be significant. However, clone 636-G had a fold value of 0.017, which means that there is 58 (1/0.017) times less template. This is likely considered significant but it really depends

on when we test these clones in assays that can give us a phenotypic expression. Also it is important to mention that the cells naturally produce OPN and therefore the amount of OPN that the cells start with can affect how we determine what is significant in term of clones that up-regulate OPN.

**Table 1**  
**Representative Clones**

Sample	Ct Value	Ct Value			
	GAPDH	OPN	OPN-GAPDH	$\Delta\Delta Ct$	fold
Parent	16.97	23.24			
Parent	16.70	22.82			
Parent		23.25			
AVG	16.84	23.10	6.27	0.00	1.00
	GAPDH	OPN	OPN-GAPDH	$\Delta\Delta Ct$	fold
6G	17.86	30.22			
6G	18.24	30.54			
6G	18.66				
AVG	18.25	30.38	12.13	5.86	0.02
	GAPDH	OPN	OPN-GAPDH	$\Delta\Delta Ct$	fold
6k	17.72	28.98			
6k	18.48	30.17			
6k	18.55	29.20			
AVG	18.25	29.58	11.32	5.06	0.03
	GAPDH	OPN	OPN-GAPDH	$\Delta\Delta Ct$	fold
FG	16.99	22.89			
FG	17.00	23.25			
FG	17.34	23.12			
AVG	17.11	23.07	5.96	-0.30	1.23

**Table 2****Up-Regulation or Down-Regulation of Clones Based on Fold Difference**

Clone cDNA	Fold Difference
parent	1
6M	0.09
6D	0.04
6G	0.02
6J	0.15
6K	0.03
6L	0.08
C1	0.82
C4	0.55
C6	0.07
FB	0.34
FC	0.18
FD	1.09
FG	1.23

\*Fold values are determined from the  $\Delta\Delta CT$  method. Generally, a fold value over 1 is considered to be significant for up-regulation and below 1 for down-regulation. For our purposes, a value of 4 is significant for up-regulation and a .01 is significant for down-regulation.

Figure 19 shows a cell migration assay with the HS766T parent cells that were not transfected. Figure 20 shows the same assay but with ASPC-1 cells. These are preliminary results from our first experiment. In the HS766T cells, the positive control shows after 48 hr that the cells are starting to close the wound but from within the center of the wound by forming aggregates. In the ASPC-1 cells, the positive control after 48 hr shows that the wound is completely closed. The negative control, with no serum and no nicotine, in both cell types shows that neither channel has been able to close the wound. At 30 nM of nicotine and no serum at 48 hr, the HS766T is starting to close the wound from the center of the channel and it resembles the positive control (Figure 19). The other concentrations of nicotine do not seem to aid in the channel closing quicker. In the ASPC-1 cells (Fig. 20), the 300 nM concentration of nicotine at 48hr shows the channel

starting to close by a projection from the side where the healthy cells remain. It is important to mention that each cancer cell line behaves differently and that is why there is a difference in how these two cells lines heal wounds.

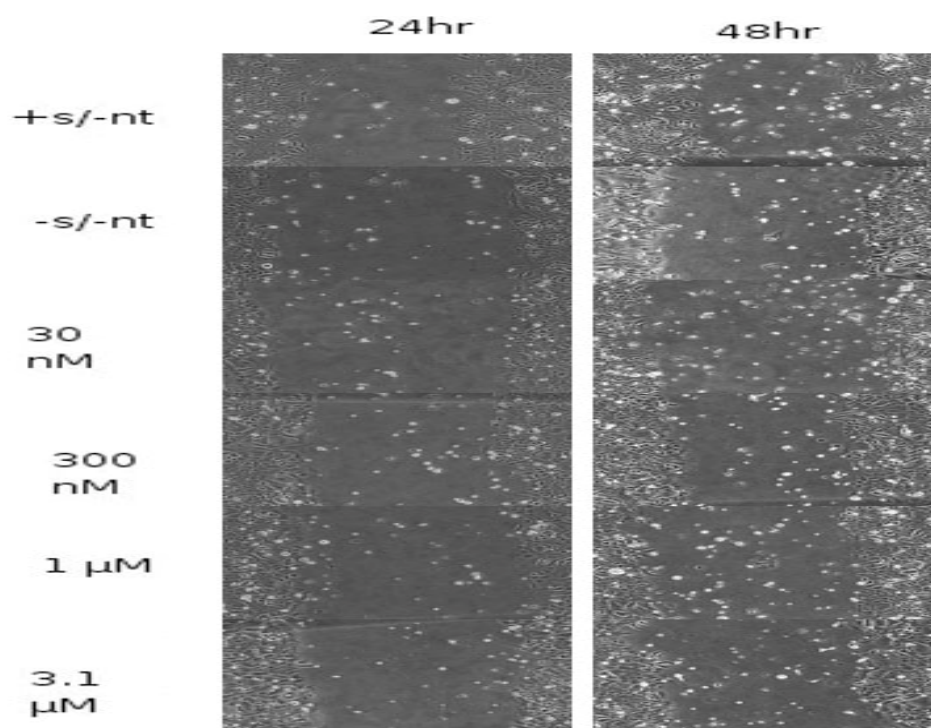


**Figure 19. Cell Migration Assay of HS766T Parent Cells.** After 48 hr, the positive control is starting to close the wound and the negative control is barely closing the wound. 30 nM of nicotine seems to be around the appropriate concentration to start to see the channel being closed by the up-regulation of OPN due to nicotine exposure. Courtesy of Tanya Gordonov.



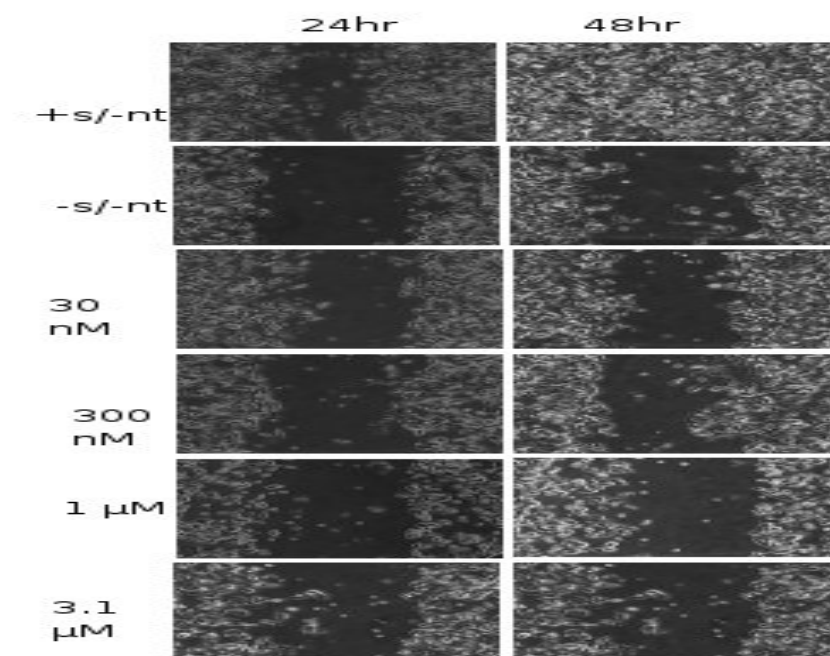


**Figure 20. Cell Migration Assay of ASPC-1 Parent Cells.** After 48hr, the positive control shows that the wound is closed and the negative control has barely closed the wound. 300 nM of nicotine seems to be around the appropriate concentration to start to see the channel being closed by the up-regulation of OPN due to nicotine exposure. Courtesy of Tanya Gordonov.

## **Chapter 4**

### **Discussion**

#### **4.1 Project 1: OPN and Characterization of anti-OPN Monoclonal Antibodies**

##### **4.1.1 OPN Characterization: Rationale**

Based on the SDS-PAGE results by Coomassie Blue and the chromatography results, there seems to be one predominant species of OPN being made by the 275-3-2 fibroblasts. This is the full-length OPNa form. To our knowledge the splice variants OPNb and OPNc are not generated in mouse cells. As previously mentioned, our method of OPN purification changed. Initially we coupled 2A1 to protein G beads, which would then bind to OPN but because of the lower yield, we changed our method to a DEAE ion-exchange chromatography. We were able to significantly increase our yield that was needed for future experiments. We were also able to make a fairly pure and stable form of OPN.

##### **4.1.2 Antibody Preparation and Characterization: Rationale**

Based on SDS-PAGE results revealed by Coomassie Blue staining and ELISA quantification, it can be seen that I purified anti-OPN monoclonal antibodies from both ascites fluid and conditioned media. Purification from conditioned media resulted in a less pure and less concentrated preparation. Also, preparations from conditioned media contained transferrin (around 75-85 kDa). When purifying antibodies made as ascites, the concentration of the antibody is higher when compared to conditioned media. Most of the hybridomas have not been cloned, a task we will undertake as we identify antibodies of interest. Clone 21B1 is of particular interest because of recent findings in our lab that it can inhibit the growth of a human melanoma line in soft agar.

Antibodies made from ascites do not have transferrin. Even though the antibodies that I worked with were all presumed to be IgGs, there were a few that had a large band around 75-85kDa. In the case of 67F7, the large band was identified as an IgM  $\mu$  chain. 67F7 made from conditioned media does have a transferrin band but the band may also be an IgM since they are both around the same molecular weight.

Five  $\mu$ g of each antibody made from ascites were used in the Coomassie Blue gel analysis done by Cassie Louis. Each band size looks very similar. For the ELISA measurements, performed by Jay Panchal, 5  $\mu$ g of OPN was coated on the plate and 1  $\mu$ l (1  $\mu$ g) of each ascites was used as the primary. The Elisa results were not consistent in terms of the Coomassie Blue results. This is to be expected since the affinity of each antibody for OPN varies. Also the avidity, which measures the overall stability of the complex between the antibody and antigen, varies as well. Avidity is governed by three major factors: intrinsic affinity of antibody for epitope, valency of antibody to antigen, and geometric arrangement of the interacting components.

## **4.2 Project 2: HUVEC Cell Survival**

### **4.2.1 Protection of HUVECs from Apoptosis by OPN**

We were successful at demonstrating a protective action of OPN on endothelial cells. In the one experiment shown once could see the difference in the wells. In the DNA content analysis, M1 peak shows the apoptotic cells (hypodiploid), the main peak are G1 phase diploid cells, and the hyperdiploid (M2) cells consist of S and G2 phase cells. The control without growth factors and no OPN had many fewer cells compared to the wells that had OPN and no growth factors. The most effective concentration of OPN was around 3ng/ml. Since protection of OPN on endothelial cells could not consistently

be reproduced, we were not able to test the effects of certain mAbs on the action of OPN. This is likely due to the variability of the physiology of the cells. I wanted to determine if certain mAbs could suppress the protection that OPN otherwise provides to growth factor-deprived endothelial cells.

Several things were tried in order to get this experiment to work. One idea was that the HUVECs may have been passaged too many times leading to impending senescence of the cells since it would take about 7 days to get a 90% confluent 10-cm plate. We also considered that the type of OPN (milk-derived hnOPN) that we were using could be ineffective. Therefore, we tried thrombin-cleaved OPN. I successfully cleaved OPN with a thrombin cleavage kit and used this cleaved OPN in the HUVEC experiments but it made no difference. The thought was that if the cryptic cleavage site was revealed that this might facilitate OPN protecting the HUVEC cells. We also tested the OPN derived from the ras-transformed mouse fibroblasts.

Maybe the results that have been seen are in part death by necrosis and not just apoptosis. In order to test this, I will next do a DNA fragmentation assay. DNA extraction followed by SDS-PAGE analysis will reveal either a smear if it is necrosis or a ladder appearance if it is apoptosis.

A cytokine assay was done for me by Guangwen Ren in Dr. Yufang Shi's lab. IL-6 and IL-8 do not show any trends but MCP-1 (Monocyte Chemotactic Protein -1) levels were increased. Other studies [Rollo et al., 1996] have also shown that OPN was most effective at a particular low concentration, becoming less effective as the concentration was either increased or decreased. Possibly this is the consequence of the ability of OPN to engage a number of distinct receptors on the cell surface. MCP-1 is a

member of the small inducible gene family (SIG) and recruits monocytes to sites of injury and infection [Gerszten et al., 1999].

#### **4.3 Project 3: Nicotine Induces OPN in Pancreatic Ductal Adenocarcinoma Cells**

The PDA cells were successfully transfected with the 636i plasmid expressing an siRNA targeting OPN, as well as the plasmids expressing OPN-FL or OPN-C designed to up-regulate the expression of OPN. About 27 clones were generated and about half of them by semi-quantitative PCR analysis showed a visual decrease or increase in the band intensity when compared to the parental cells that were not transfected. The half of the clones that looked visually promising were used in the qPCR analysis. Here absolute quantification was performed and the results were analyzed by SDS 2.0, an Applied Biosystems program. Samples that skewed the CT values significantly were removed. GAPDH was used as a housekeeping gene in order to normalize the data.

Based on the qPCR results, there were a few clones that down-regulated OPN expression. One clone of interest was Clone 6-G (636-G) that down-regulated OPN expression by 58 times less than the parent starting template. The next step will be to use the cells from the clone 6-G in a cell migration assay with and without nicotine. I will then compare the results from that assay to the same assay done with the parent cells to see if there is any phenotypic difference. There were likely no clones that successfully up-regulated OPN expression. This is probably due to that the cells normally produce endogenous OPN and therefore the amount of OPN that the cells start with can affect how we determine what is significant in term of clones that up-regulate OPN. In order to standardize this we would need to plate all cells at the same concentration and feed the

cells on the same day. That way we should be working with a similar amount of endogenous OPN.

In future research, the migration (wound healing) and invasion (Boyden Chamber) assays will be used to test the differences of the selected clones based on the qPCR analysis that positively showed up-regulation or down-regulation of OPN. The expectation is that in the presence of nicotine the cells that down-regulate OPN will be less able to close the wound because it can not induce OPN expression as much as the parent. The cells that up-regulate OPN should close the wound quicker than the parent when nicotine is added because the nicotine should increase the already up-regulated expression of OPN.

## REFERENCES

- Arafat, H., Denhardt, D. (2006). Nicotine in pancreatic cancer: Molecular mechanisms. NIH Proposal.
- Ashkenazi A. 2008. Targeting the extrinsic apoptosis pathway in cancer. *Cytokine Growth Factor Rev* 19:325-31.
- Barry ST, Ludbrook SB, Murrison E, Horgan CM. 2000. A regulated interaction between alpha5beta1 integrin and osteopontin. *Biochem Biophys Res Commun* 267:764-9.
- Bellahcene A, Castronovo V, Ogbureke KU, Fisher LW, Fedarko NS. 2008. Small integrin-binding ligand N-linked glycoproteins (SIBLINGs): multifunctional proteins in cancer. *Nat Rev Cancer* 8:212-26.
- Blum HE. 2005. Treatment of hepatocellular carcinoma. *Best Pract Res Clin Gastroenterol* 19:129-45.
- Bredesen DE, Ye X, Tasinato A, Sperandio S, Wang JJ, Assa-Munt N, Rabizadeh S. 1998. p75NTR and the concept of cellular dependence: seeing how the other half die. *Cell Death Differ* 5:365-71.
- Cao Z, Dai J, Fan K, Wang H, Ji G, Li B, Zhang D, Hou S, Qian W, Zhao J, Guo Y. 2008. A novel functional motif of osteopontin for human lymphocyte migration and survival. *Mol Immunol* 45:3683-92.
- Chambers AF, Behrend EI, Wilson SM, Denhardt DT. 1992. Induction of expression of osteopontin (OPN; secreted phosphoprotein) in metastatic, ras-transformed NIH 3T3 cells. *Anticancer Res* 12:43-7.
- Chen JJ, Jin H, Ranly DM, Sodek J, Boyan BD. 1999. Altered expression of bone sialoproteins in vitamin D-deficient rBSP2.7Luc transgenic mice. *J Bone Miner Res* 14:221-9.
- Chipitsyna G, Gong Q, Anandanadesan R, Alnajar A, Batra S, Wittel U, Cullen D, Akhter M, Denhardt D, Yeo C, Arafat H. 2009. Induction of Osteopontin by Nicotine and cigarette smoke in the pancreas and pancreatic ductal adenocarcinoma cells. *Int J of Cancer*. (In press).

Christensen B, Kazanecki CC, Petersen TE, Rittling SR, Denhardt DT, Sorensen ES. 2007. Cell type-specific post-translational modifications of mouse osteopontin are associated with different adhesive properties. *J Biol Chem* 282:19463-72.

Chung JW, Kim MS, Piao ZH, Jeong M, Yoon SR, Shin N, Kim SY, Hwang ES, Yang Y, Lee YH, Kim YS, Choi I. 2008. Osteopontin promotes the development of natural killer cells from hematopoietic stem cells. *Stem Cells* 26:2114-23.

Cook AC, Tuck AB, McCarthy S, Turner JG, Irby RB, Bloom GC, Yeatman TJ, Chambers AF. 2005. Osteopontin induces multiple changes in gene expression that reflect the six "hallmarks of cancer" in a model of breast cancer progression. *Mol Carcinog* 43:225-36.

Craig AM, Denhardt DT. 1991. The murine gene encoding secreted phosphoprotein 1 (osteopontin): promoter structure, activity, and induction in vivo by estrogen and progesterone. *Gene* 100:163-71.

Denhardt DT, Lopez CA, Rollo EE, Hwang SM, An XR, Walther SE. 1995 Osteopontin-induced modifications of cellular functions. *Ann NY Acad Sci.* 760:127-42.

Fan K, Dai J, Wang H, Wei H, Cao Z, Hou S, Qian W, Li B, Zhao J, Xu H, Yang C, Guo Y. 2008. Treatment of collagen-induced arthritis with an anti-osteopontin monoclonal antibody through promotion of apoptosis of both murine and human activated T cells. *Arthritis Rheum* 58:2041-52.

Fatherazi S, Matsa-Dunn D, Foster BL, Rutherford RB, Somerman MJ, Presland RB. 2009. Phosphate regulates osteopontin gene transcription. *J Dent Res* 88:39-44.

Fedarko NS, Jain A, Karadag A, Van Eman MR, Fisher LW. Elevated serum bone sialoprotein and osteopontin in colon, breast, prostate, and lung cancer. 2001. *Clin Cancer Res.* 12:4060-6.

Gerszten RE, Garcia-Zepeda EA, Lim YC, Yoshida M, Ding HA, Gimbrone MA, Jr., Luster AD, Luscinskas FW, Rosenzweig A. 1999. MCP-1 and IL-8 trigger firm adhesion of monocytes to vascular endothelium under flow conditions. *Nature* 398:718-23.

He B, Mirza M, Weber GF. 2006. An osteopontin splice variant induces anchorage independence in human breast cancer cells. *Oncogene* 25:2192-202.



Hijiya N, Setoguchi M, Matsuura K, Higuchi Y, Akizuki S, Yamamoto S. 1994. Cloning and characterization of the human osteopontin gene and its promoter. *Biochem J* 303 ( Pt 1):255-62.

Hotte SJ, Winkquist EW, Stitt L, Wilson SM, Chambers AF. 2002. Plasma osteopontin: associations with survival and metastasis to bone in men with hormone-refractory prostate carcinoma. *Cancer* 95:506-12.

Kazanecki, CC. 2007. Osteopontin and cell: Role of post-translational modifications and the C-terminal region. Dissertation. Rutgers University, New Brunswick, NJ.

Kazanecki CC, Kowalski AJ, Ding T, Rittling SR, Denhardt DT. 2007. Characterization of anti-osteopontin monoclonal antibodies: Binding sensitivity to post-translational modifications. *J Cell Biochem* 102:925-35.

Khan SA, Cook AC, Kappil M, Gunthert U, Chambers AF, Tuck AB, Denhardt DT. 2005. Enhanced cell surface CD44 variant (v6, v9) expression by osteopontin in breast cancer epithelial cells facilitates tumor cell migration: novel post-transcriptional, post-translational regulation. *Clin Exp Metastasis* 22:663-73.

Khan SA, Lopez-Chua CA, Zhang J, Fisher LW, Sorensen ES, Denhardt DT. 2002. Soluble osteopontin inhibits apoptosis of adherent endothelial cells deprived of growth factors. *J Cell Biochem* 85:728-36.

Lin YH, Yang-Yen HF. 2001. The osteopontin-CD44 survival signal involves activation of the phosphatidylinositol 3-kinase/Akt signaling pathway. *J Biol Chem* 276:46024-30.

Lodish H, Berk A, Kaiser C, Krieger M, Scott M, Bretscher A, Ploegh H, Matsudaira P. 2008. *Molecular Cell Biology*. Chapter 27. Immunology. W.H. Freeman and Company, New York. 6<sup>th</sup> Edition.

Luo J. 2008. Regulation of glucocorticoid synthesis by osteopontin. Honors Thesis. Rutgers University, New Brunswick, NJ.

Masuda K, Takahashi N, Tsukamoto Y, Honma H, Kohri K. 2000. N-Glycan structures of an osteopontin from human bone. *Biochem Biophys Res Commun* 268:814-7.

Mirza M, Shaughnessy E, Hurley JK, Vanpatten KA, Pestano GA, He B, Weber GF. 2008. Osteopontin-c is a selective marker of breast cancer. *Int J Cancer* 122:889-97.

- Pan HW, Ou YH, Peng SY, Liu SH, Lai PL, Lee PH, Sheu JC, Chen CL, Hsu HC. 2003. Overexpression of osteopontin is associated with intrahepatic metastasis, early recurrence, and poorer prognosis of surgically resected hepatocellular carcinoma. *Cancer* 98:119-27.
- Phillip RB, Konkol NR, Reed KM, Stein JD. 2001. Chromosome painting supports lack of homology among sex chromosomes in *Oncorhynchus*, *Salmo*, and *Salvelinus* (Salmonidae). *Genetica* 111:119-23.
- Pianezza ML, Sellers EM, Tyndale RF. 1998. Nicotine metabolism defect reduces smoking. *Nature* 393(6687):750.
- Pour PM, Runge RG, Birt D, Gingell R, Lawson T, Nagel D, Wallcave L, Salmasi SZ. 1981. Current knowledge of pancreatic carcinogenesis in the hamster and its relevance to the human disease. *Cancer* 47:1573-89.
- Rangaswami H, Bulbule A, Kundu GC. 2006. Osteopontin: role in cell signaling and cancer progression. *Trends Cell Biol* 16:79-87.
- Rollo EE, Laskin DL, Denhardt DT. 1996. Osteopontin inhibits nitric oxide production and cytotoxicity by activated RAW264.7 macrophages. *J Leukoc Biol.* 60(3):397-404.
- Saarikoski ST, Sata F, Husgafvel-Pursiainen K, Rautalahti M, Haukka J, Impivaara O, Jarvisalo J, Vainio H, Hirvonen A. 2000. CYP2D6 ultrarapid metabolizer genotype as a potential modifier of smoking behaviour. *Pharmacogenetics* 10:5-10.
- Saavedra RA, Kimbro SK, Stern DN, Schnuer J, Ashkar S, Glimcher MJ, Ljubetic CI. 1995. Gene expression and phosphorylation of mouse osteopontin. *Ann N Y Acad Sci* 760:35-43.
- Saitoh Y, Kuratsu J, Takeshima H, Yamamoto S, Ushio Y. 1995. Expression of osteopontin in human glioma. Its correlation with the malignancy. *Lab Invest* 72:55-63.
- Shevde LA, Samant RS, Paik JC, Metge BJ, Chambers AF, Casey G, Frost AR, Welch DR. 2006. Osteopontin knockdown suppresses tumorigenicity of human metastatic breast carcinoma, MDA-MB-435. *Clin Exp Metastasis* 23:123-33.
- Shinohara ML, Jansson M, Hwang ES, Werneck MB, Glimcher LH, Cantor H. 2005. T-bet-dependent expression of osteopontin contributes to T cell polarization. *Proc Natl Acad Sci USA* 102:17101-6.

Singhal H, Bautista DS, Tonkin KS, O'Malley FP, Tuck AB, Chambers AF, Harris JF. 1997. Elevated plasma osteopontin in metastatic breast cancer associated with increased tumor burden and decreased survival. *Clin Cancer Res* 3:605-11.

Sodek J, Ganss B, McKee MD. 2000. Osteopontin. *Crit Rev Oral Biol Med* 11:279-303.

Takafuji V, Forgues M, Unsworth E, Goldsmith P, Wang XW. An osteopontin fragment is essential for tumor cell invasion in hepatocellular carcinoma. 2007 *Oncogene* 44:6361-71.

Wai PY, Kuo PC. 2008. Osteopontin: regulation in tumor metastasis. *Cancer Metastasis Rev* 27:103-18.

Wajant H, Gerspach J, Pfizenmaier K. 2005. Tumor therapeutics by design: targeting and activation of death receptors. *Cytokine Growth Factor Rev* 16:55-76.

Wang X, Ford BC, Praul CA, Leach RM, Jr. 2005. Characterization of the non-collagenous proteins in avian cortical and medullary bone. *Comp Biochem Physiol B Biochem Mol Biol* 140:665-72.

Wu Y, Denhardt DT, Rittling SR. 2000. Osteopontin is required for full expression of the transformed phenotype by the ras oncogene. *Br J Cancer* 83:156-63.

Yamamoto N, Nakashima T, Torikai M, Naruse T, Morimoto J, Kon S, Sakai F, Uede T. 2007. Successful treatment of collagen-induced arthritis in non-human primates by chimeric anti-osteopontin antibody. *Int Immunopharmacol* 7:1460-70.

Ye QH, Qin LX, Forgues M, He P, Kim JW, Peng AC, Simon R, Li Y, Robles AI, Chen Y, Ma ZC, Wu ZQ, Ye SL, Liu YK, Tang ZY, Wang XW. 2003 Predicting hepatitis B virus-positive metastatic hepatocellular carcinomas using gene expression profiling and supervised machine learning. *Nat Med* 2003 (4):416-23.

Yumoto K, Ishijima M, Rittling SR, Tsuji K, Tsuchiya Y, Kon S, Nifuji A, Uede T, Denhardt DT, Noda M. 2002. Osteopontin deficiency protects joints against destruction in anti-type II collagen antibody-induced arthritis in mice. *Proc Natl Acad Sci USA*. 99(7):4556-61.

Yokosaki Y, Tanaka K, Higashikawa F, Yamashita K, Eboshida A. 2005. Distinct structural requirements for binding of the integrins  $\alpha$ v $\beta$ 6,  $\alpha$ v $\beta$ 3,  $\alpha$ v $\beta$ 5,  $\alpha$ 5 $\beta$ 1 and  $\alpha$ 9 $\beta$ 1 to osteopontin. *Matrix Biol* 24:418-27.

Zhao J, Dong L, Lu B, Wu G, Xu D, Chen J, Li K, Tong X, Dai J, Yao S, Wu M, Guo Y. 2008. Down-regulation of osteopontin suppresses growth and metastasis of hepatocellular carcinoma via induction of apoptosis. *Gastroenterology* 135:956-68.